

Unit-length Rectangular Drawings of Graphs^{*}

Carlos Alegría[✉], Giordano Da Lozzo[✉], Giuseppe Di Battista[✉],
Fabrizio Frati[✉], Fabrizio Grosso[✉], and Maurizio Patrignani[✉]

Department of Engineering, Roma Tre University, Rome, Italy
carlos.alegria@uniroma3.it, giordano.dalozzo@uniroma3.it, giuseppe.dibattista@uniroma3.it,
fabrizio.frati@uniroma3.it, fabrizio.grosso@uniroma3.it, maurizio.patrignani@uniroma3.it

Abstract. A *rectangular drawing* of a planar graph G is a planar drawing of G in which vertices are mapped to grid points, edges are mapped to horizontal and vertical straight-line segments, and faces are drawn as rectangles. Sometimes this latter constraint is relaxed for the outer face. In this paper, we study rectangular drawings in which the edges have unit length. We show a complexity dichotomy for the problem of deciding the existence of a unit-length rectangular drawing, depending on whether the outer face must also be drawn as a rectangle or not. Specifically, we prove that the problem is NP-complete for biconnected graphs when the drawing of the outer face is not required to be a rectangle, even if the sought drawing must respect a given planar embedding, whereas it is polynomial-time solvable, both in the fixed and the variable embedding settings, if the outer face is required to be drawn as a rectangle. Furthermore, we provide a linear-time algorithm for deciding whether a plane graph admits an embedding-preserving unit-length rectangular drawing if the drawing of the outer face is prescribed. As a by-product of our research, we provide the first polynomial-time algorithm to test whether a planar graph G admits a rectangular drawing, for general instances of maximum degree 4.

Keywords: Rectangular drawings · Rectilinear drawings · Matchstick graphs · Grid graphs · SPQR-trees · Planarity

1 Introduction

Among the most celebrated aesthetic criteria in Graph Drawing we have: (i) planarity, (ii) orthogonality of the edges, (iii) unit length of the edges, and (iv) convexity of the faces. We focus on drawings in which all the above aesthetics are pursued at once. Namely, we study orthogonal drawings where the edges have length one and the faces are rectangular.

Throughout the paper, any considered graph drawing has the vertices mapped at *distinct* points of the plane. Orthogonal representations are a classic research topic in Graph Drawing. A rich body of literature is devoted to orthogonal drawings of planar [17,22,26,52] and plane [14,41,42,46,47] graphs with a minimum number of bends in total or per edge [10,33,34]. An orthogonal drawing with no bend is a *rectilinear* drawing. Several papers address rectilinear drawings of planar [13,25,27,31,38,39] and plane [21,25,44,51] graphs. When all the faces of a rectilinear drawing have a rectangular shape the drawing is *rectangular*. Maximum degree-3 plane graphs admitting rectangular drawings were first characterized in [49,50]. A linear-time algorithm to find a rectangular drawing of a maximum degree-3 plane graph, provided it exists, is described in [40] and extended to maximum degree-3 planar graphs in [43]. Surveys on rectangular drawings can be found in [24,36,37]. If only the internal faces are constrained to be rectangular, then the drawing is called *inner-rectangular*. In [35] it is shown that a plane graph G has an inner-rectangular drawing T if and only if a special bipartite graph constructed from G has a perfect matching. Also, T can be found in $O(n^{1.5}/\log n)$ time if G has n vertices and a “sketch” of the outer face is prescribed, i.e., all the convex and concave outer vertices are prescribed.

^{*} This research was partially supported by PRIN projects no. 2022ME9Z78 “NextGRAAL” and no. 2022TS4Y3N “EXPAND”. A preliminary version of this research has appeared in the Proceedings of the 30th International Symposium on Graph Drawing and Network Visualization [2].

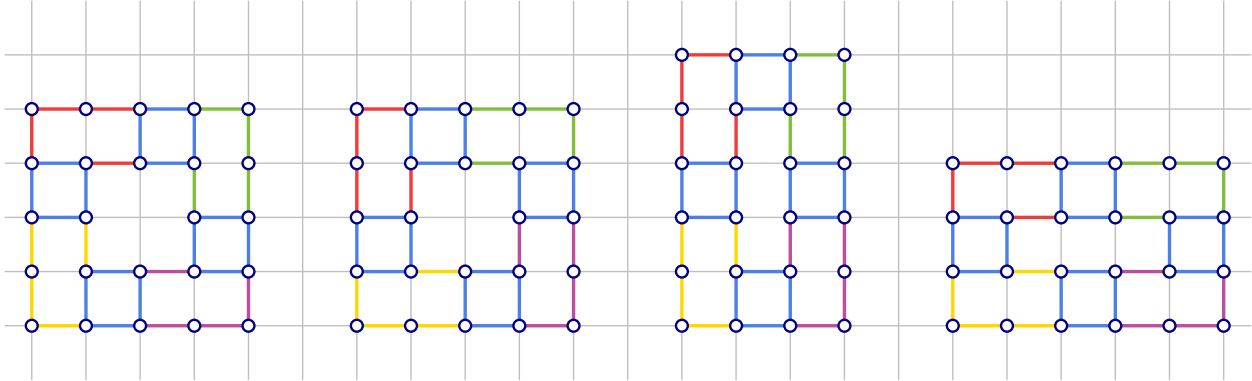


Fig. 1. Unit-length embedding-preserving rectangular drawings of a plane graph.

Computing straight-line drawings whose edges have constrained length is another core topic in graph drawing [1,3,4,7,12,23,45]. The graphs admitting planar straight-line drawings with all edges of the same length are also called *matchstick graphs*. Recognizing matchstick graphs is NP-hard for biconnected [23] and triconnected [12] graphs, and in fact, even strongly $\exists\mathbb{R}$ -complete [1]; see also [45].

A *unit-length grid drawing* maps vertices to grid points and edges to horizontal or vertical segments of unit Euclidean length. A *grid graph* is a graph that admits a unit-length grid drawing¹. Recognizing grid graphs is NP-complete for ternary trees of pathwidth 3 [9], for binary trees [28], and for trees of pathwidth 2 [29], but solvable in polynomial time on graphs of pathwidth 1 [29]. A variant of the grid graph recognition problem is when the drawing is constrained to be contained in the $k \times r$ grid. In [29] this problem is shown to be NP-hard when $k = 3$ even on graphs of pathwidth 2. The same problem is shown to be fixed-parameter tractable (FPT) parameterized by $k + m_{cc}$, where m_{cc} is the maximum size of a connected component of G . An exponential-time algorithm to compute, for a given weighted planar graph, a rectilinear drawing in which the Euclidean length of each edge is equal to the edge weight has been presented in [7].

Let G be a planar graph. The UNIT-LENGTH INNER-RECTANGULAR DRAWING RECOGNITION (for short, UIR) problem asks whether a unit-length inner-rectangular drawing of G exists. Similarly, the UNIT-LENGTH RECTANGULAR DRAWING RECOGNITION (for short, UR) problem asks whether a unit-length rectangular drawing of G exists. Let now H be a plane or planar embedded (i.e., no outer face specified) graph. The UNIT-LENGTH INNER-RECTANGULAR DRAWING RECOGNITION WITH FIXED EMBEDDING (for short, UIRFE) problem asks whether a unit-length inner-rectangular embedding-preserving drawing of H exists. Similarly, the UNIT-LENGTH RECTANGULAR DRAWING RECOGNITION WITH FIXED EMBEDDING (for short, URFE) problem asks whether a unit-length rectangular embedding-preserving drawing of H exists; Fig. 1 shows different unit-length rectangular drawings of the same plane graph.

Our contribution. In Sect. 3 we show NP-completeness for the UIRFE (Theorem 1) and UIR (Theorem 2) problems when the input graph is biconnected, which is surprising since a biconnected graph has degrees of freedom that are more restricted than those of a tree. In Sect. 4 we provide a linear-time algorithm for the UIRFE and URFE problems if the drawing of the outer face is given (Theorem 3). In Sect. 5 we first show that the URFE problem is cubic-time solvable; the time bound becomes linear if all internal faces of the input graph have maximum degree 6. These results hold both when the outer face is prescribed (Theorem 4) and when it is not (Theorem 5). Second, we show a necessary condition for an instance of the UR problem to be positive in terms of its SPQR-tree (Lemma 4). Exploiting the above condition, we show that the UR problem is cubic-time solvable; the running time becomes linear when the SPQR-tree of the input graph satisfies special conditions (Theorem 6). Finally, as a by-product of our research, we provide the

¹ Note that in some literature the term “grid graph” denotes an “induced” graph, i.e., there is an edge between any two vertices at distance one. See, for example, [32].

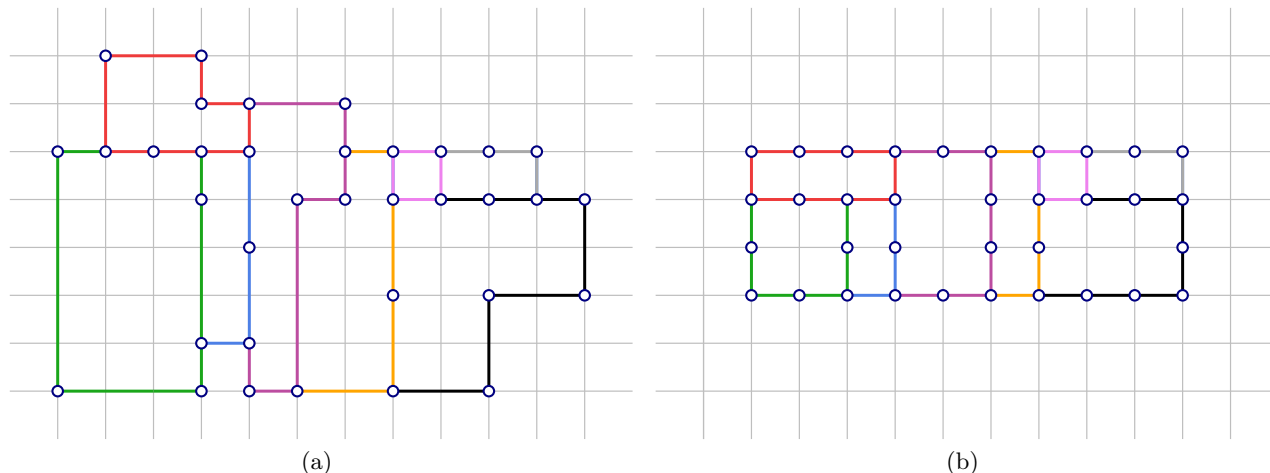


Fig. 2. (a) A planar rectilinear grid drawing of a graph. (b) A unit-length rectangular grid drawing of the same graph.

first polynomial-time algorithm to test whether a planar graph G admits a rectangular drawing, for general instances of maximum degree 4 (Theorem 7).

2 Preliminaries

For basic graph drawing terminology and definitions refer, e.g., to [16,36].

Drawings and embeddings. A *drawing* of a graph maps each vertex to a distinct point on the plane and each edge to a Jordan arc connecting its end-vertices. A drawing of a graph is *planar* if it contains no vertex-edge overlaps and no edge-edge crossings. A planar drawing of a graph partitions the plane into topologically connected regions called *faces*. The unbounded face is called the *outer face*. Two planar drawings of a connected graph are *planar equivalent* if they induce the same counter-clockwise ordering of the edges incident to each vertex. Also, they are *plane equivalent* if they are planar equivalent and the clockwise order of the edges along the boundaries of their outer faces is the same. The equivalence classes of planar equivalent drawings are called *planar embeddings*, whereas the equivalence classes of plane equivalent drawings are called *plane embeddings*. A *planar embedded graph* is a planar graph equipped with one of its planar embeddings. Similarly, a *plane graph* is a planar graph equipped with one of its plane embeddings. Given a planar embedded (resp. plane) graph G and a planar (resp. plane) embedding \mathcal{E} of G , a planar drawing Γ of G is *embedding-preserving* if $\Gamma \in \mathcal{E}$. Consider a planar graph G . If G is connected, a planar embedding of G is defined by the counter-clockwise circular order of the edges incident on each vertex, while a plane embedding of G is defined by the counter-clockwise circular order of the edges incident on each vertex and by the choice of the outer face. Instead, if G is not connected, then a planar (plane) embedding is defined by a planar (plane) embedding of each of its connected components, together with the relative placement of each of these components to one another, called *relative positions*, which specifies an assignment of each connected component to one face of each other component.

Geometric definitions A *polygon* is a closed polygonal chain consisting of a finite number of straight-line segments. A polygon *intersects itself* if two segments non-adjacent in the chain have a non-void intersection. A polygon is *simple* if it does not intersect itself. This implies that there are no repeated segments or points in the chain. A polygon is *weakly simple* if it bounds a region of the plane that is homeomorphic to an open disk. A simple polygon is *convex* if its interior is a convex set. A *convex drawing* of a planar graph G is a straight-line planar drawing of G in which all the faces are drawn as convex polygons, including the outer

face. In [20], it has been shown that a planar graph admits a convex drawing only if it is biconnected. A *convex subdivision* of a simple polygon P is partition of the interior of P into convex sets. Note that a convex drawing defines a convex subdivision of the polygon bounding the outer face.

Unit-length rectangular drawings. A *rectilinear drawing* of a graph is a drawing such that each edge is an horizontal or vertical straight-line segment; see Fig. 2(a). An *inner-rectangular* drawing is a rectilinear drawing such that all its faces, except possibly for the outer face, are drawn as rectangles. An inner-rectangular drawing is *rectangular* if its outer face is drawn as rectangle. In a *grid drawing*, vertices are mapped to points with integer coordinates (i.e., *grid points*). A drawing of a graph in which all edges have unit Euclidean length is a *unit-length drawing* (see Fig. 2(b) for an example).

Observation 1. *A unit-length grid drawing is rectilinear and planar.*

Observation 2. *A unit-length rectangular (or inner-rectangular) drawing is planar and it is a grid drawing, up to a rigid transformation.*

The following simple property has been proved in [6, Lemma 1].

Property 1. Every cycle that admits a unit-length grid drawing has even length.

Since (inner) rectangular drawings exist only for maximum-degree-4 graphs, in the remainder, we assume that all considered graphs satisfy this requirement.

Connectivity. Let G be a graph. A *cut-vertex* (resp. *separation pair*) in a graph G is a vertex (resp. a pair of vertices) whose removal disconnects G . Graph G is *biconnected* (*triconnected*) if it has no cut-vertex (resp. no separation pair). A *biconnected component* (or *block*) of a graph G is a maximal (in terms of vertices and edges) biconnected subgraph of G . A block is *trivial* if it consists of a single edge and *non-trivial* otherwise. A *split pair* of G is either a pair of adjacent vertices or a separation pair. The *components of G with respect to a split pair $\{u, v\}$* are defined as follows. If (u, v) is an edge of G , then it is a component of G with respect to $\{u, v\}$. Also, let G_1, \dots, G_k be the connected components of $G \setminus \{u, v\}$. The subgraphs of G induced by $V(G_i) \cup \{u, v\}$, minus the edge (u, v) , are components of G with respect to $\{u, v\}$, for $i = 1, \dots, k$.

2.1 SPQR-trees

We provide details of the SPQR-tree data structure introduced by Di Battista and Tamassia [18,19] to handle all planar embeddings of a biconnected planar graph H . The SPQR-tree T of H represents a decomposition of H into triconnected components along its split pairs. Each node μ of T is associated with a graph, called *skeleton of μ* , and denoted by $\text{sk}(\mu)$. The edges of $\text{sk}(\mu)$ are either edges of H , which we call *real edges*, or newly introduced edges, called *virtual edges*. The tree T is initialized to a single node μ , whose skeleton, composed only of real edges, is H . Consider a split pair $\{u, v\}$ of the skeleton of some node μ of T , and let H_1, \dots, H_k be the components of H with respect to $\{u, v\}$ such that H_1 is not a single virtual edge and, if $k = 2$, also H_2 is not a single virtual edge. We introduce a node ν adjacent to μ whose skeleton is the graph $H_1 + e_{\nu, \mu}$, where $e_{\nu, \mu} = (u, v)$ is a virtual edge; also, we replace the skeleton $\text{sk}(\mu)$ of μ with the graph $\bigcup_{i \neq 1} H_i + e_{\mu, \nu}$, where $e_{\mu, \nu} = (u, v)$ is a virtual edge. We say that $e_{\nu, \mu}$ is the *twin virtual edge of $e_{\mu, \nu}$* , and vice versa. Applying this replacement iteratively produces a tree with more nodes but smaller skeletons associated with the nodes. Eventually, when no further replacement is possible, the skeletons of the nodes of T are of four types: parallels of at least three virtual edges (*P-nodes*), parallels of exactly one virtual edge and one real edge (*Q-nodes*), cycles of exactly three virtual edges (*S-nodes*), and triconnected planar graphs (*R-nodes*). The *merge* of two adjacent nodes μ and ν in T , replaces μ and ν in T with a new node τ that is adjacent to all the neighbors of μ and ν , and whose skeleton is $\text{sk}(\mu) \cup \text{sk}(\nu) \setminus \{e_{\mu, \nu}, e_{\nu, \mu}\}$, where the end-vertices of $e_{\mu, \nu}$ and $e_{\nu, \mu}$ that correspond to the same vertices of H are identified. By iteratively merging adjacent *S-nodes*, we eventually obtain the (unique) SPQR-tree data structure as introduced by Di Battista and Tamassia [18,19], where the skeleton of an *S-node* is a cycle. The crucial property of this decomposition is that a planar embedding of H uniquely induces a planar embedding of the skeletons of its nodes and

that, arbitrarily and independently, choosing planar embeddings for all the skeletons uniquely determines an embedding of H . Observe that the skeletons of S - and Q -nodes have a unique planar embedding, that the skeleton of R -nodes have two planar embeddings (which are one the reflection of the other), and that P -nodes have as many planar embedding as the permutations of their virtual edges. Consider a node ν and a virtual edge $e_{\nu,\mu}$ in $\text{sk}(\nu)$. Among the subtrees of T obtained by removing the arc (ν, μ) from T , let $T_{\nu,\mu}$ be the one that contains ν . The *expansion graph* $\text{exp}(e_{\nu,\mu})$ of $e_{\nu,\mu}$ is the subgraph of H obtained by iteratively merging all the nodes in $T_{\nu,\mu}$ and by removing the virtual edge $e_{\nu,\mu}$.

It is often convenient to orient the arcs of T so that, in the resulting directed tree, one Q -node ρ is a sink and all other nodes have exactly one outgoing arc. Such an orientation corresponds to rooting T at ρ , and we call it a *normal orientation* of T . The next definitions assume a normal orientation of T . For a node $\mu \neq \rho$ of T , the *poles* of μ are the endpoints of the virtual edge $e_{\nu,\mu}$ of $\text{sk}(\mu)$ where ν is the parent of μ ; whereas the poles of ρ are the endpoints of its unique virtual edge. Consider any plane embedding \mathcal{E} of H in which the real edge corresponding to ρ is incident to the outer face. Then \mathcal{E} yields a plane embedding \mathcal{E}_μ of the skeleton of each node μ of T in which the poles of μ are also incident to the outer face of \mathcal{E}_μ . This motivates the next definitions. Consider a node $\mu \neq \rho$. Also, let u and v be the poles of μ . Let ν be the parent of μ and let $e_{\mu,\nu}$ be the virtual edge representing μ in $\text{sk}(\nu)$. Let \mathcal{E}_μ be the restriction of \mathcal{E} to $\text{exp}(e_{\mu,\nu})$ and let H_μ be the corresponding plane graph. Note that there exist exactly two faces of \mathcal{E} that are incident to edges of the outer face of H_μ . We call such faces the *outer faces* of \mathcal{E}_μ . By convention, we call *left outer face* $\ell(\mathcal{E}_\mu)$ of \mathcal{E}_μ (*right outer face* $r(\mathcal{E}_\mu)$ of \mathcal{E}_μ) the outer face that is delimited by the path obtained by walking in clockwise direction (resp. in counter-clockwise direction) from u to v along the boundary of the outer face of \mathcal{E}_μ . The terms left outer face and right outer face come from the fact that we usually think about \mathcal{E}_μ as having the pole u at the bottom and the other pole v at the top.

If H has n vertices, then T has $O(n)$ nodes and the total number of virtual edges in the skeletons of the nodes of T is in $O(n)$. From a computational complexity perspective, T can be constructed in $O(n)$ time [30].

3 NP-completeness of the UIRFE and UIR problems

In this section we show NP-completeness for both the UIRFE and UIR problems when the input graph is biconnected. Observe that both problems clearly lie in NP, as a certificate for a biconnected n -vertex input graph consists of an injective mapping from the vertices of the graph to the points of a grid whose sides have length bounded by $\frac{n}{2}$. In fact, it is possible to verify in polynomial-time whether such a mapping defines a unit-length rectangular drawing, and in the positive case whether it respects a given planar embedding. Therefore, in the remainder of the section, we will focus on establishing polynomial-time reductions to show the NP-hardness of the problems. We start with the following theorem.

Theorem 1. *The UNIT-LENGTH INNER-RECTANGULAR DRAWING RECOGNITION WITH FIXED EMBEDDING problem is NP-complete, even for biconnected plane graphs whose internal faces have maximum size 6.*

Let ϕ be a Boolean formula in conjunctive normal form with at most three literals in each clause. We denote by G_ϕ the *incidence graph* of ϕ , i.e., the graph that has a vertex for each clause of ϕ , a vertex for each variable of ϕ , and an edge (c, v) for each clause c that contains the *positive literal* v or the *negated literal* \bar{v} . The formula ϕ is an instance of PLANAR MONOTONE 3-SAT if G_ϕ is planar and each clause of ϕ is either positive or negative. A *positive clause* contains only positive literals, while a *negative clause* contains only negated literals. Hereafter, w.l.o.g., we assume that all the clauses of ϕ contain *exactly* three literals. In fact, a clause with less than three literals can be modified by duplicating one of the literals in the clause, without altering the satisfiability of ϕ . Note that this modification might turn G_ϕ into a planar multi-graph.

A *monotone rectilinear representation* of G_ϕ is a drawing that satisfies the following properties (refer to Fig. 3(a)).

- P1:** Variables and clauses are represented by axis-aligned rectangles with the same height.
- P2:** The bottom sides of all rectangles representing variables lie on the same horizontal line.
- P3:** The rectangles representing positive (resp. negative) clauses lie above (resp. below) the rectangles representing variables.

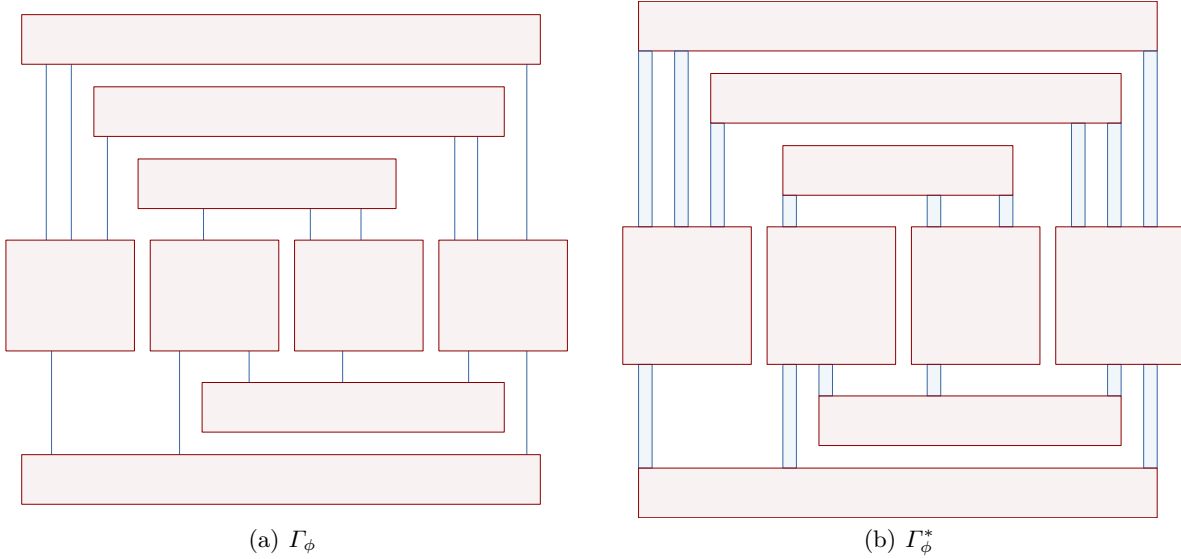


Fig. 3. (a) A monotone rectilinear representation Γ_ϕ of G_ϕ . The rectangles representing variables and clauses are red, whereas the line segments and rectangles representing the edges of ϕ are blue. (b) The auxiliary representation Γ_ϕ^* that satisfies the properties D1 to D5.

P4: Edges connecting variables and clauses are represented by vertical segments.

P5: The drawing is crossing-free.

The PLANAR MONOTONE 3-SAT problem is known to be NP-complete, even when the incidence graph G_ϕ of ϕ is provided along with a monotone rectilinear representation Γ_ϕ of G_ϕ [8]. We prove Theorem 1 by showing how to construct a plane graph H_ϕ that is biconnected, has internal faces of maximum size 6, and admits a unit-length inner-rectangular drawing *if and only if* ϕ is satisfiable. Our strategy is to modify Γ_ϕ to create a suitable auxiliary representation Γ_ϕ^* (see Fig. 3) and then to use the geometric information of Γ_ϕ^* as a blueprint to construct H_ϕ . We provide below a high-level description of the logic behind the reduction.

3.1 The auxiliary monotone rectilinear representation Γ_ϕ^*

Hereafter, let δ_ϕ^+ (resp. δ_ϕ^-) be the maximum degree of G_ϕ when restricted to nodes representing variables and positive (resp. negative) clauses. Let $\delta_\phi = \max(\delta_\phi^+, \delta_\phi^-)$. We denote by $|\phi|$ the size of ϕ , that is, the number of variables plus the number of clauses in the formula. The auxiliary representation has the following properties (refer to Fig. 3):

D1: The variables, clauses, and edges of G_ϕ are represented by axis-aligned rectangles whose corners have integer coordinates, i.e., they lie at grid points.

D2: The width and height of the bounding box of Γ_ϕ^* are polynomially bounded in $|\phi|$.

D3: The rectangles representing variables have $O(\delta_\phi)$ width, constant height, and their bottom sides lie on a common horizontal grid line.

D4: Each rectangle representing a clause has $O(|\phi| \cdot \delta_\phi)$ width and constant height.

D5: Each rectangle representing an edge has constant width and $O(|\phi|)$ height.

We can obtain Γ_ϕ^* by suitably translating and scaling the rectangles that represent the variables, clauses, and edges of ϕ in Γ_ϕ . Clearly, these transformations can be done in polynomial time in $|\phi|$. We obtain the following lemma.

Lemma 1. *Starting from Γ_ϕ , the representation Γ_ϕ^* can be constructed in polynomial time in $|\phi|$.*

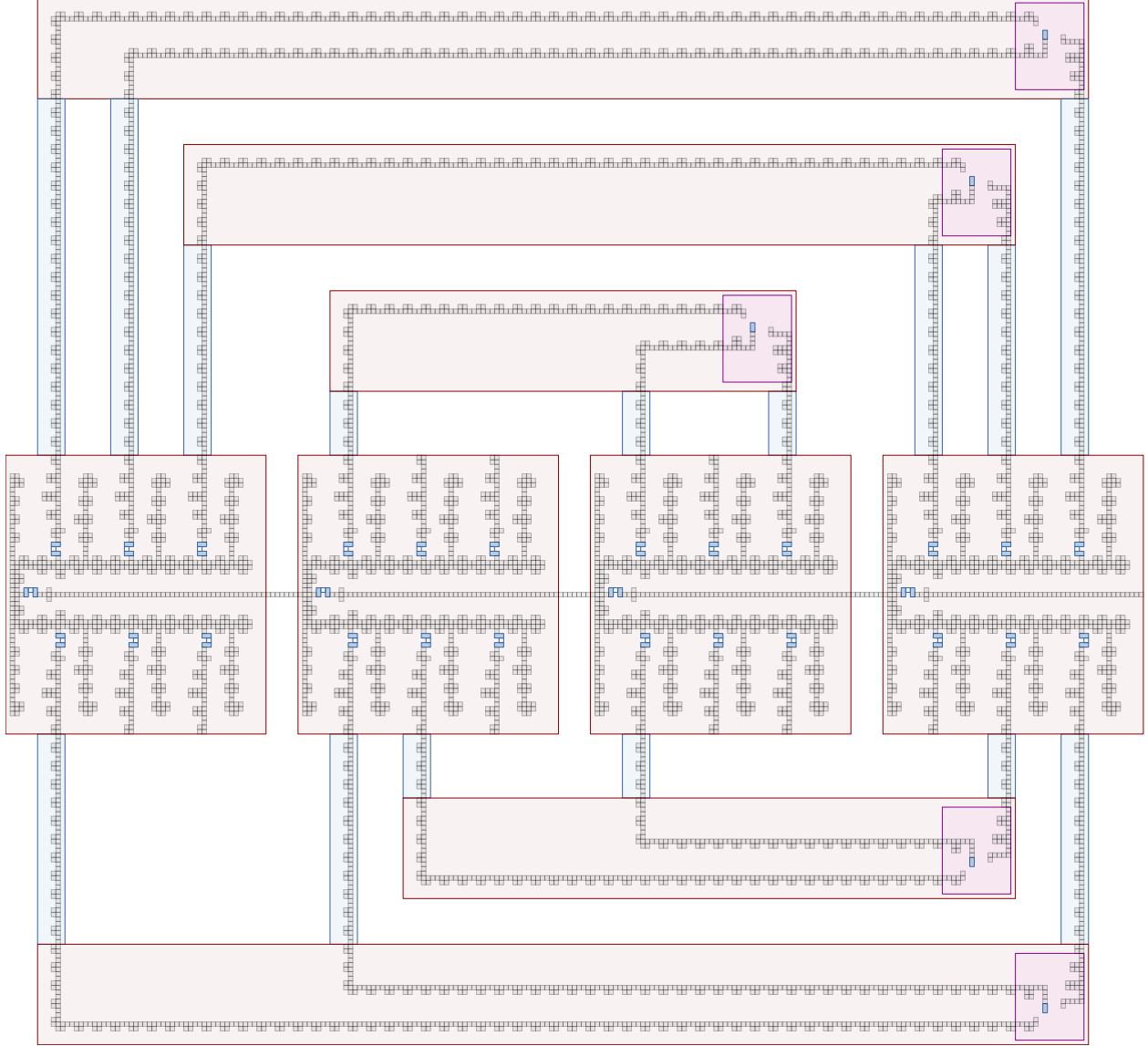


Fig. 4. The graph H_ϕ , with some faces omitted. Variable and clause gadgets are enclosed in light red boxes, while transmission gadgets are enclosed in light blue boxes.

Overview of the reduction. The reduction is based on three main types of gadgets. A variable $v \in \phi$ is modeled by means of a *variable gadget*, a clause $c \in \phi$ by means of an (α, β) -*clause gadget*, and an edge $(v, c) \in G_\phi$ by means of a λ -*transmission gadget*. We use the geometric properties of Γ_ϕ^* to determine the size and structure of each gadget, as well as how to combine the gadgets together to form H_ϕ . In particular, we use the distances between the rectangles representing edges and clauses to compute the auxiliary parameters α , β and λ , which in turn are used to construct (α, β) -clause gadgets and λ -transmission gadgets. Finally, the incidences between the rectangles representing variables, edges, and clauses are used to decide how to join the edges of the gadgets to construct a biconnected graph.

An example of a unit-length inner-rectangular drawing of H_ϕ is shown in Fig. 4; some faces of H_ϕ are omitted. All these missing faces are part of *domino components*, which admit a constant number of unit-length inner-rectangular drawings, see Fig. 5; some of these faces are shown filled in white or blue in Fig. 4.

Detailed illustrations of the variable, (α, β) -clause, and λ -transmission gadgets are in Figs. 6 to 8, respectively. In these figures, the enclosing rectangles of the gadgets are also included, as well as the faces of H_ϕ missing on Fig. 4, which are shown in blue.

The logic behind the construction is as follows. Consider the illustration of a variable gadget shown in Fig. 6. A variable gadget admits two unit-length inner-rectangular drawings. These drawings differ from each other on whether the domino components cross the bottom (Fig. 6(a)) or the top (Fig. 6(b)) side of the red enclosing rectangle, and correspond to a **true** and a **false** value assignment to the associated variable, respectively. The truth assignments are propagated from variable to clause gadgets via λ -transmission gadgets. The illustration of a λ -transmission gadget is shown in Fig. 7. Consider the auxiliary interior purple rectangle R . A λ -transmission gadget is modeled in such a way that if a domino component sticking out of a variable gadget forces the bottom-most (resp. top-most) domino component to lie inside R , then there is a domino component crossing the top (resp. bottom) side of R . In turn, the crossing domino component propagates the truth assignment by forcing a drawing of the domino components of the adjacent (α, β) -clause gadget. An illustration of an (α, β) -clause gadget is shown in Fig. 8. An (α, β) -clause gadget is designed in such a way that it admits a unit-length inner-rectangular drawing if and only if the drawings of its three incident λ -transmission gadgets allow for at least one domino component to cross the red rectangle.

3.2 Description of the gadgets

All the gadgets have internal faces of size either 4 or 6, and are formed by two sets of special subgraphs we call the *frames* and the *domino components*. A frame is a biconnected subgraph formed by internal faces of size 4, and has a unique unit-length inner-rectangular drawing (up to rigid transformations). A domino component is instead a biconnected subgraph with internal faces of size either 4 or 6. We define three different types of domino components: the L-shape, the C-shape, and the Stick. Such components have constantly many unit-length inner-rectangular drawings, shown in Fig. 5. However, the geometry of the construction will force the L-shape components to have either the first or the last unit-length inner-rectangular drawing in Fig. 5(a) and the C-shape components to have either the first or the last unit-length inner-rectangular drawing in Fig. 5(c).

Variable Gadget. Variable gadgets are formed by $2\delta_\phi + 2$ frames connected together by means of C-shape components, and a set of L-shape and stick components to propagate the truth assignment of the corresponding variable. Refer to Fig. 6 for an illustration of the gadget.

Let \mathcal{V} denote the variable gadget modeling some variable $v \in \phi$. There are three crucial properties of the variable gadget. First, C-shape components are adjacent to frames in such a way that in every unit-length inner-rectangular drawing of \mathcal{V} the drawing of the frames of \mathcal{V} is the same. This implies that the bounding box \mathcal{B} of the drawing of the frames of \mathcal{V} does not change, regardless of the drawings of the C-shape components. Second, \mathcal{V} admits two unit-length inner-rectangular drawings that we associate with the **true** (Fig. 6(a)) and **false** (Fig. 6(b)) truth assignments of v . We remark that in the drawing corresponding to the **true** (resp. **false**) assignment, there are δ_ϕ L-shape components crossing the bottom (resp. top) side of \mathcal{B} . Finally, the gadget is constructed in such a way that the width and height of \mathcal{B} are the same as those of the rectangle of Γ_ϕ^* representing v .

λ -transmission Gadget. The λ -transmission gadget is formed by a single frame, and a set of $\lfloor (\lambda - 2)/4 \rfloor$ L-shape components to propagate truth assignments from variable to clause gadgets. Refer to Fig. 7 for an illustration of the gadget.

Let \mathcal{L} denote the λ -transmission gadget modeling some edge (v, c) of G_ϕ that connects a variable v to a clause c . Consider the auxiliary purple rectangle R , and the L-shape components labeled with L_D and L_U in Fig. 7. There are two crucial properties of the λ -transmission gadget. First, in any unit-length inner-rectangular drawing of \mathcal{L} , if L_D does not cross R then L_U crosses R , and vice versa. Observe that, if an L-shape component of a variable gadget crosses the top (resp. bottom) side of its red enclosing rectangle, then L_U (resp. L_D) crosses R . This is how the truth assignment for a variable gets propagated through

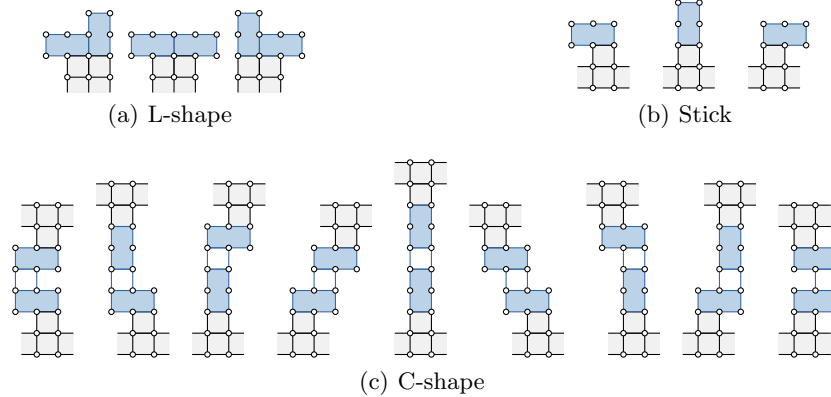


Fig. 5. The unit-length grid drawings of the domino components. Frame faces are filled gray. Domino component faces are filled blue (size 6) and white (size 4).

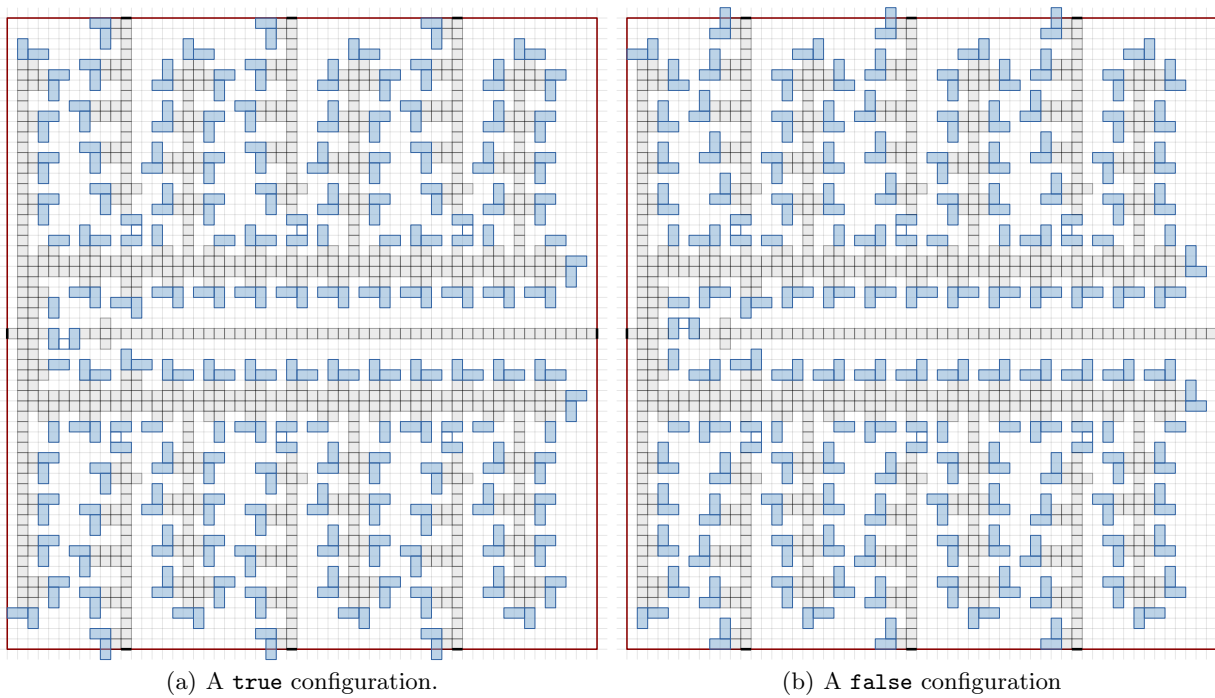


Fig. 6. The variable gadget.

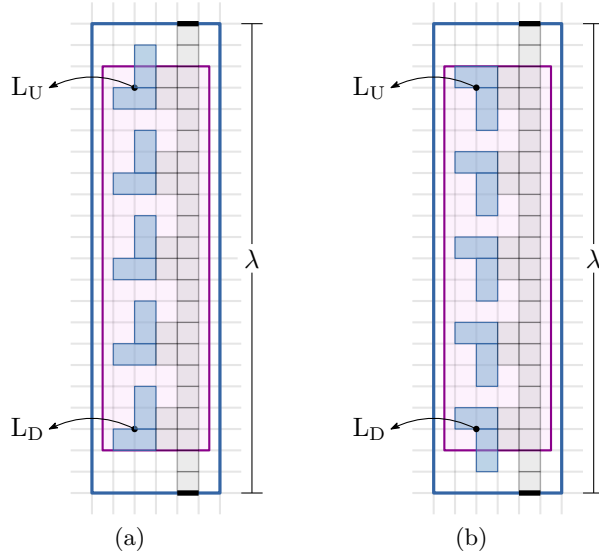


Fig. 7. Unit-length inner-rectangular drawings of a λ -transmission gadget for $\lambda = 22$. (a) If L_D does not cross the purple rectangle, then L_U crosses the purple rectangle. (b) If L_U does not cross the purple rectangle, then L_D crosses the purple rectangle.

transmission gadgets. Second, the width and height of the bounding box \mathcal{B} of all the unit-length inner-rectangular drawings of \mathcal{L} are the same. Moreover, the width and height of \mathcal{B} are less than or equal to the width and height of the rectangle of Γ_ϕ^* representing (v, c) .

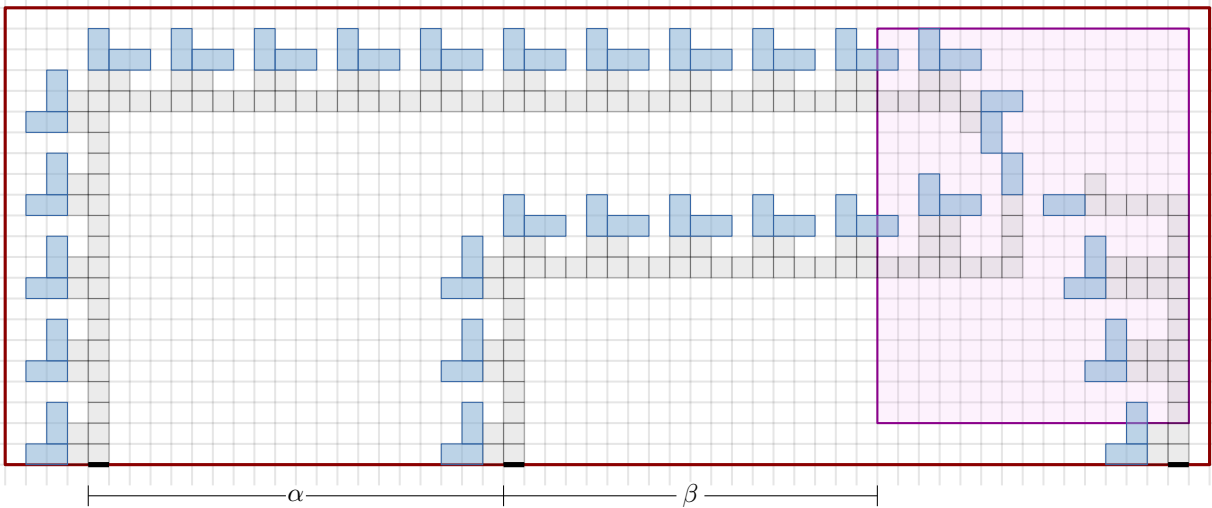
(α, β)-clause Gadget. In the following, refer to the example drawings of an (α, β) -clause gadget shown in Fig. 8. Let \mathcal{C} denote the (α, β) -clause gadget modeling a clause $c \in \phi$. Let R denote the auxiliary purple rectangle shown in Fig. 8. The gadget \mathcal{C} is formed by three disconnected components. Each component is formed by a frame that, in the final graph H_ϕ , is connected to the frame of a λ -transmission gadget modeling an edge of G_ϕ incident to c . The components are also equipped with L-shape components to propagate the truth assignments coming from λ -transmission gadgets.

Consider for the moment the three connected subgraphs of \mathcal{C} that admit a unit-length inner-rectangular drawing lying outside R . Note that they are straightforward extensions of λ -transmission gadgets. These auxiliary gadgets are used to propagate to R the truth assignments coming from the boundary of the red enclosing rectangle. Each auxiliary gadget has the property that, in any unit-length inner-rectangular drawing, if no L-shape component crosses the red enclosing rectangle, then there is one L-shape component crossing R .

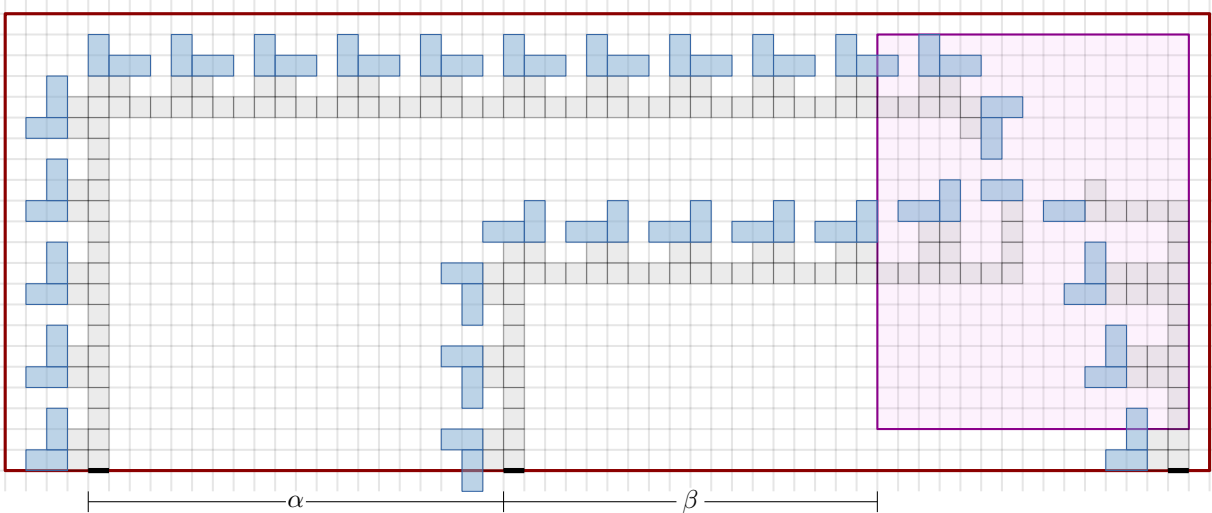
Consider now the subgraphs of \mathcal{C} that admit a unit-length inner-rectangular drawing lying in the interior of R . The logic of the gadget is implemented by these subgraphs via the following crucial property: \mathcal{C} admits a unit-length inner-rectangular drawing if and only if at least one L-shape component of the auxiliary gadgets is not crossing R . See for example Fig. 8(a) in which all the three L-shape components of the auxiliary gadgets cross R , hence the (α, β) -clause gadget does not admit a unit-length inner-rectangular drawing.

3.3 Combining the gadgets together to form H_ϕ

For the purpose of combining two gadgets into a single connected graph, every gadget provides a set of special edges called *attachment edges*. In Figs. 6 to 8, the attachment edges are shown as thick black segments. To combine two gadgets together, we first identify one attachment edge in each gadget, and then join the attachment edges together so that there is a single edge shared by both gadgets.



(a) The gadget admits no unit-length inner-rectangular drawing in which no L-shape component crosses the red rectangle.



(b) The gadget admits a unit-length inner-rectangular drawing in which at least one L-shape component crosses the red rectangle.

Fig. 8. The (α, β) -clause gadget. The values of α and β employed in the picture are smaller than they should be, for the sake of visibility.

In the following description, the properties D1-D5 of Γ_ϕ^* are exploited to guarantee that, after combining all the gadgets, H_ϕ admits a unit-length inner-rectangular drawing if and only if ϕ is satisfiable. To obtain H_ϕ , we start by constructing the variable gadgets as above. The variable gadgets are connected together by means of frames, each consisting of a sequence of a constant number of faces of size 4, so that only faces that are consecutive in the sequence share vertices. Each of such frames is combined with two variable gadgets by means of the attachment edges lying on the right and the left sides of their red enclosing rectangles. The process continues by constructing a λ -transmission gadget for each edge of G_ϕ . The value of the parameter λ of each gadget is the height of the blue rectangle of Γ_ϕ^* representing the associated edge of G_ϕ . A λ -transmission gadget and a variable gadget are combined together joining an attachment edge lying on the

top (resp. bottom) side of the red enclosing rectangle of the variable gadget, and the attachment edge lying on the bottom (resp. top) side of the blue enclosing rectangle of the λ -transmission gadget. We finally construct an (α, β) -clause gadget for each clause of ϕ . We select the parameters α and β according to the width of the red rectangles representing clauses in Γ_ϕ^* , and the horizontal distances between the blue rectangles representing the edges incident to the modeled clause. A λ -transmission gadget and an (α, β) -clause gadget are combined together joining an attachment edge lying on the bottom (resp. top) side of the red enclosing rectangle of the (α, β) -clause gadget, and the attachment edge lying on the top (resp. bottom) side of the blue enclosing rectangle of the λ -transmission gadget.

By the construction described above, it is not hard to see that H_ϕ is biconnected and admits a unit-length inner-rectangular drawing that preserves the given plane embedding if and only if ϕ is satisfiable. The crucial property is that the domino components we use are forced to admit a constant number of unit-length inner-rectangular drawings that are all embedding preserving; see again Fig. 5.

By showing that the graph H_ϕ only admits unit-length inner-rectangular drawings that preserve the same plane embedding, we get the following.

Theorem 2. *The UNIT-LENGTH INNER-RECTANGULAR problem is NP-complete, even for biconnected planar graphs that admit an embedding in which the internal faces have maximum size 6.*

Proof. We show that the graph H_ϕ only admits unit-length inner-rectangular drawings that preserve the same plane embedding. Let Γ and Γ' be two unit-length inner-rectangular drawings of H_ϕ . By construction, every edge of H_ϕ belongs to at least a length-4 or a length-6 chordless cycle. Each such a cycle must necessarily bound an internal face of Γ and Γ' . Therefore, the cycle bounding the outer face of Γ and Γ' is the same. Let us call the cycles bounding the internal faces of Γ and Γ' the *inner cycles* of H_ϕ . By construction, any inner cycle shares at least an edge with another inner cycle. Therefore, the orientation of the inner cycles is the same in Γ as in Γ' (up to a reflection of the entire drawing). Therefore, all the unit-length inner-rectangular drawings admitted by H_ϕ preserve the same plane embedding, which is unique up to reflections of the whole drawing. \square

Since any unit-length grid drawing of a cycle with 4 or 6 vertices is a rectangle, the previous theorem implies the following result.

Corollary 1. *It is NP-complete to decide whether a biconnected planar graph G admits a unit-length grid drawing, even if G has a prescribed plane embedding.*

4 An Algorithm for the UIRFE and URFE Problems with a Prescribed Drawing of the Outer Face

In this section, we show a linear-time algorithm for the UIRFE (and consequently for the URFE) problem in the case in which the drawing of the outer face is prescribed.

We start with two auxiliary lemmata. The first one is an extension of a classical result by Devillers et al. [15].

Lemma 2. *Let G be a connected planar graph and \mathcal{E} be a plane embedding of G . A straight-line drawing Γ of G is planar and respects \mathcal{E} if and only if:*

- for every face f of \mathcal{E} , the walk delimiting f is represented in Γ by a weakly simple polygon, whose orientation is as prescribed by \mathcal{E} ;
- for every vertex v of G , the clockwise order of the edges incident to v in Γ is the same as in \mathcal{E} ; and
- let C_o be the walk delimiting the outer face f_o of \mathcal{E} , and let Γ_o be the weakly simple polygon representing C_o in Γ ; then every edge not in C_o that is incident to a vertex v of C_o , leaves v towards the interior of Γ_o .

Proof. The necessity is obvious. We prove the sufficiency. Suppose hence that Γ satisfies the properties described in the statement. We prove that it is planar and respects \mathcal{E} .

Let ρ_h be equal to $3n - h - 3$. Note that ρ_h is the number of edges of a biconnected internally-triangulated n -vertex plane graph whose outer face is delimited by a cycle with h vertices. We prove the lemma by induction on $\rho_k - |E(G)|$, where the index k is the number of vertices of the convex hull of Γ_o .

If $\rho_k - |E(G)| = 0$, then each internal face of \mathcal{E} is delimited by a 3-cycle and C_o is a k -cycle. Since (i) each internal face of \mathcal{E} is delimited in Γ by a triangle, and C_o is represented in Γ by a convex k -gon, and since (ii) the clockwise order of the edges incident to each vertex in Γ is as prescribed by \mathcal{E} , a classic result by Devillers et al. [15, Lemma 19] implies that Γ is planar and induces a convex subdivision Γ of Γ_o (that also respects the planar embedding of G obtained by disregarding the choice of the outer face of \mathcal{E}). Finally, the fact that G is connected and that every edge not in C_o that is incident to a vertex of C_o leaves this vertex toward the interior of Γ_o implies that Γ_o bounds the outer face of Γ , and thus Γ respects (the plane embedding) \mathcal{E} .

Let us now consider the case in which $\rho_k - |E(G)| > 0$. Let f be a face of \mathcal{E} such that either f is an internal face of \mathcal{E} of length at least 4 or $f = f_o$ if the polygon Γ_o bounding f_o in Γ is not convex. Then it is possible to draw in f a straight-line segment \overline{uv} between some pair of vertices u and v incident to f , such that \overline{uv} does not cross any edge of f . In particular, \overline{uv} divides f into two faces f' and f'' . Let G' be the plane graph obtained from G by introducing the edge (u, v) so that it splits the face f into the faces f' and f'' . To define a plane embedding \mathcal{E}' for G' , it only remains to specify a choice for its outer face. If $f \neq f_o$, then f_o is the outer face of \mathcal{E}' . Otherwise, the outer face of \mathcal{E}' is the unbounded face between f' and f'' . Let Γ' be the drawing of G' obtained from Γ by drawing the edge (u, v) as the straight-line segment \overline{uv} .

Observe that $\rho_k - |E(G')| < \rho_k - |E(G)|$. Furthermore, all the conditions of the statement are satisfied by Γ' , \mathcal{E}' , and G' . Therefore, by induction, Γ' is planar and respects \mathcal{E}' . The fact that the restriction of Γ' to G yields a planar drawing Γ of G that respects \mathcal{E} concludes the proof. \square

Lemma 3. *Let G be a plane graph and let Γ_o be a unit-length grid drawing of the outer face f_o of G . Then, an embedding-preserving inner-rectangular unit-length drawing of G in which f_o is delimited by Γ_o , if any, is unique.*

Proof. First, we can assume that G is connected. Indeed, if it is not, then the relative positions of distinct connected components of G are such that each connected component lies in the outer face of each other, as otherwise obviously G would not admit any inner-rectangular drawing and there would be nothing to prove. It follows that Γ_o specifies a unit-length grid drawing of the outer face of each connected component of G and thus it suffices to prove the lemma for an individual connected component of G in order to prove it for G itself. So in the rest of the proof we assume that G is connected. We denote by $b(f)$ the walk of G that bounds a face f . Note that, for any internal face f , $b(f)$ must be a simple cycle, as otherwise G does not have a unit-length embedding-preserving inner-rectangular drawing.

We prove the lemma by induction on the number i of internal faces of G . If $i = 1$, then G coincides with the cycle $b(f_o)$ and it admits a unit-length embedding-preserving inner-rectangular drawing if and only if Γ_o is a rectangle oriented as prescribed by the embedding of G .

If $i > 1$, then consider a vertex v incident to f_o with minimum x -coordinate in Γ_o . Let f be any internal face of G incident to v and let P_{left} be the subgraph of G induced by the vertices of G with minimum x -coordinate in Γ_o . Observe that, if P_{left} is not a collection of (chordless) paths, then G does not admit a unit-length embedding-preserving inner-rectangular drawing in which f_o is delimited by Γ_o , and the statement trivially holds. Let now $P_{\text{left}}(f) := P_{\text{left}} \cap b(f)$ be the subgraph of P_{left} induced by the vertices on the boundary of f . If $P_{\text{left}}(f)$ consists of multiple connected components, then f cannot be drawn as a rectangle in any unit-length embedding-preserving inner-rectangular drawing of G in which f_o is delimited by Γ_o , and the statement trivially holds. In fact, since $v \in P_{\text{left}}(f)$, we have that the drawing of the left side of a rectangle R representing f must coincide with the drawing of $P_{\text{left}}(f)$. This in turn implies that R is *prescribed*, that is, the rectangle R representing $b(f)$ in an embedding-preserving inner-rectangular unit-length drawing of G in which f_o is delimited by Γ_o is univocally determined. Clearly, G does not admit a unit-length embedding-preserving inner-rectangular drawing in which f_o is delimited by Γ_o if **(F1)** R places

a vertex in $V(f) \setminus V(f_o)$ on top of vertices in $V(f_o) \setminus V(f)$ or if **(F2)** R assigns a vertex on $V(f) \cap V(f_o)$ different coordinates than the ones prescribed by Γ_o . If any of such conditions holds, then the statement trivially holds. Suppose now that neither (F1) nor (F2) occurs, and let Γ'_o be the drawing obtained from Γ_o by removing the edges of $P_{\text{left}}(f)$ and all the resulting isolated vertices, if any. Similarly, let G' be the plane graph obtained by removing from G all the edges of $P_{\text{left}}(f)$ and all the resulting isolated vertices, if any. Note that G' is the plane subgraph of G whose internal faces are the faces of G different from f and whose outer face f'_o is obtained by merging f_o and f , which is achieved by removing the edges and vertices of $P_{\text{left}}(f)$ except for its end-vertices. Also, note that Γ'_o is a unit-length grid drawing of f'_o . Therefore, since G' contains $i - 1$ internal faces, we can now apply induction. The following two cases are possible. **Case 1:** G' does not admit a unit-length embedding-preserving inner-rectangular drawing in which f'_o is delimited by Γ'_o . In this case, G does not admit a unit-length embedding-preserving inner-rectangular drawing in which f_o is delimited by Γ_o , and the statement holds. **Case 2:** Let Γ' be the unique unit-length embedding-preserving inner-rectangular drawing of G' in which f'_o is delimited by Γ'_o ; note that, since we are not in **Case 1**, such a drawing exists and is unique by the inductive hypothesis. Clearly, by adding R to Γ' we obtain a unit-length embedding-preserving inner-rectangular drawing of G in which f_o is delimited by Γ_o , which is unique since the drawing of R is prescribed and since Γ' is unique. This concludes the proof. \square

Consider a connected instance of the UIRFE problem, i.e., an n -vertex connected plane graph G ; let \mathcal{E} be the plane embedding prescribed for G . Let Γ_o be a unit-length grid drawing of the walk bounding the outer face f_o of \mathcal{E} . W.l.o.g, assume that the smallest x - and y - coordinates of the vertices of Γ_o are equal to 0. Next, we describe an $O(n)$ -time algorithm, called **RECTANGULAR-HOLES ALGORITHM**, to decide whether G admits a unit-length inner-rectangular drawing that respects \mathcal{E} and in which the walk bounding f_o is represented by Γ_o .

We first check whether each internal face of \mathcal{E} is bounded by a simple cycle of even length, as otherwise the instance is negative by Property 1. This can be trivially done in $O(n)$ time. We remove from G the bridges incident to the outer face and the resulting isolated vertices.

Now the algorithm processes the internal faces of G one at a time. When a face f is considered, the algorithm either detects that G is a negative instance or assigns x - and y - coordinates to all the vertices of f . In the latter case, we say that f is *processed* and its vertices are *placed*. Since the drawing of f_o is prescribed, at the beginning each vertex incident to f_o is placed, while the remaining vertices are not. Also, every internal face of \mathcal{E} is not processed. The algorithm concludes that the instance is negative if one of the following conditions holds: **(C1)** there is a placed vertex to which the algorithm tries to assign coordinates different from those already assigned to it, or **(C2)** there are two placed vertices with the same x -coordinate and the same y -coordinate. If neither Condition C1 nor C2 occurs, after processing all the internal faces the vertex placement provides a unit-length inner-rectangular drawing of the input instance.

To process faces, the algorithm maintains some auxiliary data structures:

- A **graph** H , called the **CURRENT GRAPH**, which is the subgraph of G composed of the vertices and of the edges incident to non-processed (internal) faces. Initially, we have $H = G$. In particular, we will maintain the invariant that each biconnected component of H is non-trivial. We will also maintain the outer face of the restriction \mathcal{E}_H of \mathcal{E} to H , which we will still denote by f_o . When the current graph is H , all the vertices incident to the outer face of \mathcal{E}_H are already placed, i.e., the drawing of each cycle delimiting the outer face of a biconnected component of H is determined.
- An **array** A , called the **CURRENT OUTER-SORTER**, that contains $M_x + 1$ buckets, each implemented as a double-linked list, where M_x is the largest x -coordinate of a vertex in Γ_o . The bucket $A[i]$ contains the placed vertices of H (i.e., those incident to the outer face of H) whose x -coordinate is equal to i . Moreover, A is equipped with the index x_{\min} of the first non-empty bucket. To allow removals of vertices in $O(1)$ time, we enrich each placed vertex with x -coordinate i with a pointer to the corresponding list-item in the list $A[i]$.
- A **set of pointers** for the edges of H : Each edge (u, v) is equipped with two pointers ℓ_{uv} and ℓ_{vu} , that reference the faces of \mathcal{E} lying to the left of (u, v) , when traversing such an edge from u to v and from v to u , respectively.

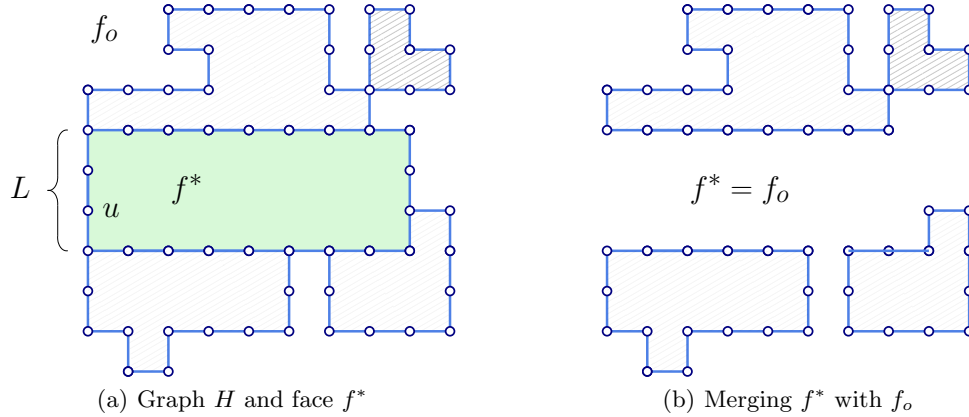


Fig. 9. A step of the RECTANGULAR-HOLES ALGORITHM.

At each iteration the algorithm performs the following steps; see Fig. 9. **Retrieve:** It retrieves an internal face f^* with at least one vertex u with minimum x -coordinate (i.e., x_{\min}) among the placed vertices of H ; such a vertex is incident to the outer face of H . **Draw:** It assigns coordinates to all the vertices incident to f^* in such a way that f^* is drawn as a rectangle R^* . Note that such a drawing is unique. Indeed, in any embedding-preserving inner-rectangular unit-length drawing of H in which the cycle delimiting the outer face of each biconnected component of H is the one prescribed, the left side of R^* coincides with the maximal path L containing u that is induced by the placed vertices of f^* with x -coordinate equal to x_{\min} . **Merge:** It merges f^* with f_o by suitably changing the pointers of every edge incident to f^* , and by removing each edge (u, v) incident to f^* with pointers $\ell_{uv} = \ell_{vu} = f_o$, as well as any resulting isolated vertex. Further, it updates A consequently. Note that, after the merge step, the outer face f_o of the new current graph H is again completely drawn.

4.1 Details of the Retrieve, Draw, and Merge Steps

We now describe each step in detail.

Retrieve f^* . We take the first vertex u in the non-empty bucket $A[x_{\min}]$. Since u has the smallest x -coordinate among the placed vertices of H , then u is incident to f_o . Furthermore, since the blocks of H are non-trivial, u has degree either two, three or four in H .

Consider first the case in which u has degree 4. Since u is a vertex with smallest x -coordinate in H and it is incident to f_o , its neighbors must be placed with x -coordinates greater than or equal to x_{\min} . This is not possible since it would imply that two neighbors of u are drawn on the same grid point. Hence, Condition C2 holds and the algorithm stops giving a negative result.

Consider now the case in which u has degree either two or three (refer to Fig. 9(a)). Let f^* be any (of the at most two) internal faces of H incident to u . Let L denote the maximal path containing u that is induced by all the placed vertices of f^* with x -coordinate x_{\min} . Note that the edges of L are incident to f_o , and must form the left side of the rectangle R^* representing f^* in the unit-length grid drawing of H with the given drawing of f_o . Moreover, since all the vertices of the outer face of H have x -coordinate greater than or equal to x_{\min} , such side determines the coordinates of all the vertices of f^* along R^* .

Draw f^* . We traverse the vertices of f^* while assigning the coordinates determined in the previous step to each vertex. If there is a vertex of f^* for which Condition C1 holds, we conclude that the instance is negative, and terminate the algorithm. Otherwise, each newly placed vertex that was assigned the x -coordinate i is inserted at the beginning of $A[i]$ (observe that the vertices placed before drawing f^* are already in A).

Merge f^* with f_o . We traverse counter-clockwise f^* and, for each edge (u, v) that is traversed from u to v , we set ℓ_{uv} to point to f_o . Then, we remove from H each edge (u, v) with $\ell_{vu} = \ell_{uv} = f_o$ as well as all the resulting isolated vertices, if any (see Fig. 9(b)). To finish this step we remove from A all the vertices that were removed from H , and update x_{\min} , if necessary.

The proof of the next theorem exploits the RECTANGULAR-HOLES ALGORITHM.

Theorem 3. *The UNIT-LENGTH INNER-RECTANGULAR FIXED-EMBEDDING and UNIT-LENGTH FIXED EMBEDDING problems are $O(n)$ -time solvable for an n -vertex plane graph if the drawing of the outer face is prescribed.*

Proof. First, as noted previously, it suffices to look at a connected plane graph, as distinct connected components can be dealt with independently. Indeed, the relative positions of such components in the prescribed plane embedding force them to be one outside the other, as otherwise the plane graph would not admit any embedding-preserving inner-rectangular drawing. This implies that the drawing of the outer face is prescribed for each of such components.

In order to prove the theorem, we argue about the correctness and running time of the RECTANGULAR-HOLES ALGORITHM.

We start with the correctness. Consider that, if the algorithm terminates without a failure, then, by construction, (i) each internal face of G has been drawn as a rectangle, (ii) the rotation system of each vertex has been respected, and (iii) the edges incident to vertices of the cycle delimiting the outer face are drawn as line segments leaving such a cycle towards the interior of the prescribed drawing of the outer face. Thus, by Lemma 2, the drawing is planar. Again by construction, the coordinates of the vertices on the outer face have not been changed and the edges are horizontal or vertical segments of unit length, hence the drawing is a unit-length grid drawing.

Otherwise, if a failure condition is reached, then we prove that G does not admit any embedding-preserving unit-length grid drawing where each internal face is drawn as a rectangle and the drawing of the outer face is as prescribed. Assume that the algorithm fails due to Condition C1, i.e., the algorithm is forced to assign different coordinates to the same vertex. Since by Lemma 3 if the drawing exists it is unique, then the instance does not admit a grid realization with the prescribed properties. Assume instead that the algorithm fails due to Condition C2, i.e., the algorithm is forced to assign the same coordinates to different vertices. This would imply that the drawing is not planar, in contradiction with Lemma 2.

We finally prove that the RECTANGULAR-HOLES ALGORITHM runs in $O(n)$ time. The algorithm performs as many iterations as the internal faces of G . At each iteration on a face f^* , it performs a number of operations that is linear in the number of vertices and edges of f^* . Hence, each edge is processed constant number of times, and each vertex is considered at most as many times as the number of incident faces, i.e., at most four times. \square

Theorem 3 contrasts with the NP-hardness results of Theorems 1 and 2, where the drawing of the outer face is not prescribed. By again exploiting the observation that any unit-length grid drawing of a cycle with 4 or 6 vertices is a rectangle, Theorem 3 implies the following result.

Corollary 2. *Deciding whether a biconnected plane graph admits a unit-length grid drawing is a linear-time solvable problem if the drawing of the outer face is prescribed and all the internal faces have maximum degree 6.*

5 Algorithms for the URFE and UR problems

In this section we study the UNIT-LENGTH RECTANGULAR problem. Since rectangular drawings are convex, the input graphs for the UR problem must be biconnected [20].

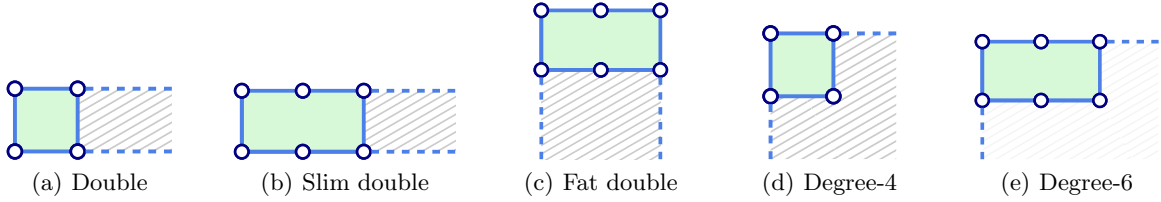


Fig. 10. Corner faces for the proof of Theorem 4.

Fixed Embedding. We start by considering instances with either a prescribed plane embedding (Theorem 4) or a prescribed planar embedding (Theorem 5).

Theorem 4. *The UNIT-LENGTH FIXED EMBEDDING problem is cubic-time solvable for a plane graph G and it is linear-time solvable if all internal faces of G have maximum degree 6.*

Proof. If the input is not biconnected, then we can determine that the instance is negative in linear time [48]. Hence, in the following, we assume that the input is biconnected, which implies that any face is bounded by a cycle.

In order to solve the URFE problem in polynomial time, we guess all the possible rectangular grid drawings of the outer face f_o . For each of them we invoke Theorem 3. We have that the rectangular grid drawings of f_o are in one-to-one correspondence (up to a rotation of 90° , 180° , or 270°) with the possible choices of two vertices that become consecutive corners of the drawing. This corresponds to $O(n^2)$ choices for the drawing of f_o . For each choice the algorithm RECTANGULAR-HOLES ALGORITHM finds a unit-length grid rectangular drawing in $O(n)$ time, if it exists.

Assume now that all internal faces have maximum degree 6. Our strategy is to efficiently determine the drawing of the outer face of the input graph G and then to invoke Theorem 3 to conclude the proof.

Note that, if G is a 4-cycle or a 6-cycle, then the instance is trivially positive. We henceforth assume this is not the case. We have also the following simple cases.

- A *double corner face* is a degree-4 face with three edges incident to f_o , see Fig. 10(a).
- A *slim double corner face* is a degree-6 face with five edges incident to f_o , see Fig. 10(b).
- A *fat double corner face* is a degree-6 face with four edges incident to f_o , see Fig. 10(c).

If G has a double, slim double, or fat double corner face, then such a face must provide two consecutive 270° angles incident any realization of f_o as a rectangle, hence the drawing of the outer face is prescribed and RECTANGULAR-HOLES ALGORITHM can be invoked.

Suppose now that none of the aforementioned cases holds. A *corner face* is a degree-4 face that has two edges incident to the outer face f_o , see Fig. 10(d), or a degree-6 face that has three edges incident to f_o , see Fig. 10(e). Observe that, by the assumption that there is no double, slim double, or fat double corner face, a face is incident to a corner of a rectangular drawing of f_o if and only if it is a corner face. Hence, there must be exactly four corner faces in order for a rectangular drawing of the input instance to exist, otherwise the input instance is negative. The four corner faces can be trivially found in $O(n)$ time. They determine a constant number of possible drawings of the outer face as follows. If a corner face has degree-4, then its degree-2 vertex must be a corner of the drawing of the outer face. If a corner face has instead degree-6, then one of its two degree-2 vertices must be a corner of the drawing of the external face. Hence we have at most $2^4 = O(1)$ different possible choices for the drawing of the outer face. We solve the URFE problem in this setting by invoking RECTANGULAR-HOLES ALGORITHM with each choice as the prescribed drawing of the outer face of G . \square

By showing that any planar embedding has a unique candidate outer face supporting a unit-length rectangular drawing, we get the following.

Theorem 5. *The UNIT-LENGTH FIXED EMBEDDING problem is cubic-time solvable for a planar embedded graph G , and it is linear-time solvable if all but at most one face of G have maximum degree 6.*

Proof. Observe that, given two rectangles R_1 and R_2 , a necessary condition for drawing R_2 inside R_1 is that the perimeter of R_2 is smaller than the perimeter of R_1 . Hence, given a connected planar embedded graph G , we first compute the faces of G with the maximum number of edges in linear time. Suppose that there exists exactly one face f_o with the maximum number of edges. We invoke Theorem 4 for checking in cubic time (linear, if all the faces different from f_o have degree 6) if the plane graph consisting of G with the prescribed outer face f_o is a positive or negative instance of URFE. Suppose now that there exists more than one face with the maximum number of edges. If G is just an even-length simple cycle, then we conclude that G is a positive instance of URFE. Otherwise, we conclude the opposite. \square

Variable Embedding. Now, we turn our attention to instances with a variable embedding. We start by providing some relevant properties of the graphs that admit a rectangular (not necessarily unit-length or grid) drawing. Let G be one such graph. To avoid degenerate cases, in what follows, we assume that G is not a cycle, a special case which can be dealt with separately. Let Γ be a rectangular drawing of G and let Γ_o be the rectangle delimiting the outer face of Γ . Refer to Fig. 11. Consider the plane graph G_Γ corresponding to Γ . Since Γ is convex, then G_Γ is a subdivision of an *internally triconnected* plane graph [5, Theorem 1]. That is, every separation pair $\{u, v\}$ of G_Γ is such that u and v are incident to the outer face and each connected component of $G_\Gamma \setminus \{u, v\}$ contains a vertex incident to the outer face.

Consider a separation pair $\{u, v\}$ of G . In the following, we provide several useful properties related to $\{u, v\}$.

Property 2. If at least one of u and v is not in Γ_o , then there exist exactly two components of G with respect to $\{u, v\}$, one of which is a simple path. Also, the vertices of such a path are drawn on a straight line. See, e.g., the vertices x_1 and y_1 in Fig. 11.

Proof. The first part of the statement is a consequence of the fact that G is a subdivision of an internally-triconnected plane graph. The second part, instead, follows immediately from the fact that Γ is rectangular. \square

Property 3. If both u and v are in Γ_o , then there exist either two or three components of G with respect to $\{u, v\}$.

Proof. The statement follows from the fact that, since u and v are in Γ_o and since Γ_o is drawn as a rectangle, their degree is at most 3. \square

Property 4. If both u and v are in Γ_o and G has three components G_1 , G_2 , and G_3 with respect to $\{u, v\}$, then there is exactly one component, say G_2 , such that $G_2 \setminus \{u, v\}$ does not contain vertices in Γ_o . Also, G_2 is a simple path whose vertices are drawn on a straight line. Furthermore, u and v are drawn on opposite sides of Γ_o . Finally, we have that each of u and v has degree 1 both in G_1 and in G_3 . See, e.g., the vertices x_2 and y_2 in Fig. 11.

Proof. The component G_2 must be a simple path, since G is a subdivision of an internally-triconnected plane graph. Also, the vertices of such a path must be drawn either along a horizontal or a vertical line, as otherwise Γ would not be rectangular. Finally, since u and v are incident to the outer face and since they both have degree 1 in G_2 , we have that each of u and v has degree 1 both in G_1 and in G_3 . \square

Property 5. There exist no two separation pairs $\{u_1, v_1\}$ and $\{u_2, v_2\}$ of G such that u_1 and v_1 lie on opposite sides of Γ_o , u_2 and v_2 lie on the opposite side of Γ_o , and u_1 and u_2 lie on perpendicular sides of Γ_o .

Proof. Suppose for a contradiction that there exist two separation pairs $\{u_1, v_1\}$ and $\{u_2, v_2\}$ of G with the properties in the statement. Then there exists an internal face f_1 of Γ incident to u_1 and to v_1 , and an internal face f_2 of Γ incident to u_2 and to v_2 . However, since Γ is rectangular, this is possible only if $f_1 = f_2$, which contradicts the assumption that G is not a cycle. \square

Property 6. If both u and v are in Γ_o and G has two components G_1 and G_2 with respect to $\{u, v\}$ such that (i) both G_1 and G_2 are not simple paths in G , and (ii) both u and v have degree 2 in G_1 , then u and v are drawn on opposite sides of Γ_o and G_1 contains a path P_1 between u and v , whose vertices are on a straight line, that is incident to an internal face of Γ . See, e.g., the vertices x_3 and y_3 in Fig. 11.

Proof. Note that each of u and v is incident to an internal edge that belongs to G_1 (possibly the edge (u, v)) and each such edge must be incident to the same internal face f of Γ . Since f is rectangular, the vertices of the subpath P_1 of f connecting u and v and passing through these edges must be drawn along a straight line. To complete the proof, we observe that this implies that u and v must be drawn on opposite sides of Γ_o . \square

The next properties follow directly from the fact that Γ is rectangular.

Property 7. Suppose that G has two components G_1 and G_2 with respect to $\{u, v\}$. If u and v are on the same side of Γ_o , then exactly one of G_1 and G_2 is a path whose vertices lie in Γ_o on a straight line. See, e.g., the vertices x_4 and y_4 in Fig. 11.

Property 8. Suppose that G has two components G_1 and G_2 with respect to $\{u, v\}$. If u and v are incident to perpendicular sides of Γ_o , then exactly one of G_1 and G_2 , say G_1 , is a simple path. Moreover, G_1 is drawn in Γ as an orthogonal polygonal line with a single bend. See, e.g., the vertices x_5 and y_5 in Fig. 11.

Property 9. Suppose that G has two components G_1 and G_2 with respect to $\{u, v\}$. If u and v are on opposite sides of Γ_o , then each of u and v has degree 1 in at least one of G_1 and G_2 . See, e.g., the vertices x_6 and y_6 in Fig. 11.

A *caterpillar* is a tree such that removing its leaves results in a path, called *spine*, possibly composed of a single node. The *pruned SPQR-tree* of a biconnected planar graph G , denoted by T^* , is the tree obtained from the SPQR-tree T of G , after removing the Q -nodes of T .

Lemma 4. *Let G be a graph that admits a rectangular drawing. Then the pruned SPQR-tree T^* of G is a caterpillar with the following properties:*

- (i) *All its leaves are S -nodes;*
- (ii) *its spine contains no two adjacent R -nodes;*
- (iii) *its spine contains no two adjacent nodes μ and ν such that μ is a P -node and ν is an R -node;*
- (iv) *each P -node μ has exactly 3 neighbors in T ; and*
- (v) *the skeleton of each S -node of the spine of T^* contains two chains of virtual edges corresponding to Q -nodes, separated by two virtual edges, each corresponding to either a P - or an R -node.*

Proof. In the following, we assume that G is not a cycle, as otherwise the statement trivially holds. With this assumption, T^* contains at least one P - or R -node.

Let Γ be a rectangular drawing of G , and let Γ_o be the drawing of the outer face of Γ . Refer to Fig. 11.

Suppose, for a contradiction, that there exist two adjacent R -nodes μ and ν in the spine of T^* . Let $\{u, v\}$ be the separation pair shared by their skeletons, and let $e_{\mu, \nu}$ and $e_{\nu, \mu}$ be the virtual edges in $\text{sk}(\nu)$ and in $\text{sk}(\mu)$ corresponding to μ and to ν , respectively. By Property 2, both u and v must lie in Γ_o . By Properties 7 and 8, u and v must lie on opposite sides of Γ_o . Therefore, by Property 9, each of u and v has degree 1 in at least one of $\text{exp}(e_{\mu, \nu})$ and $\text{exp}(e_{\nu, \mu})$, which implies that either μ or ν is an S -node. Therefore, we get a contradiction. This proves **Condition (ii)** of the statement.

By Property 2, the poles of a P -node of T are incident to Γ_o . By Property 4, the neighbors of a P -node are either S - or Q -nodes. This proves **Condition (iii)**.

A P -node μ of T has at least three neighbors in T , by definition. By Properties 2 and 3, we have that any node of T has at most three neighbors in T . This proves **Condition (iv)**.

Next, we show that T^* is a caterpillar, and that it satisfies **Conditions (i)** and **(v)** of the statement. We distinguish two cases.

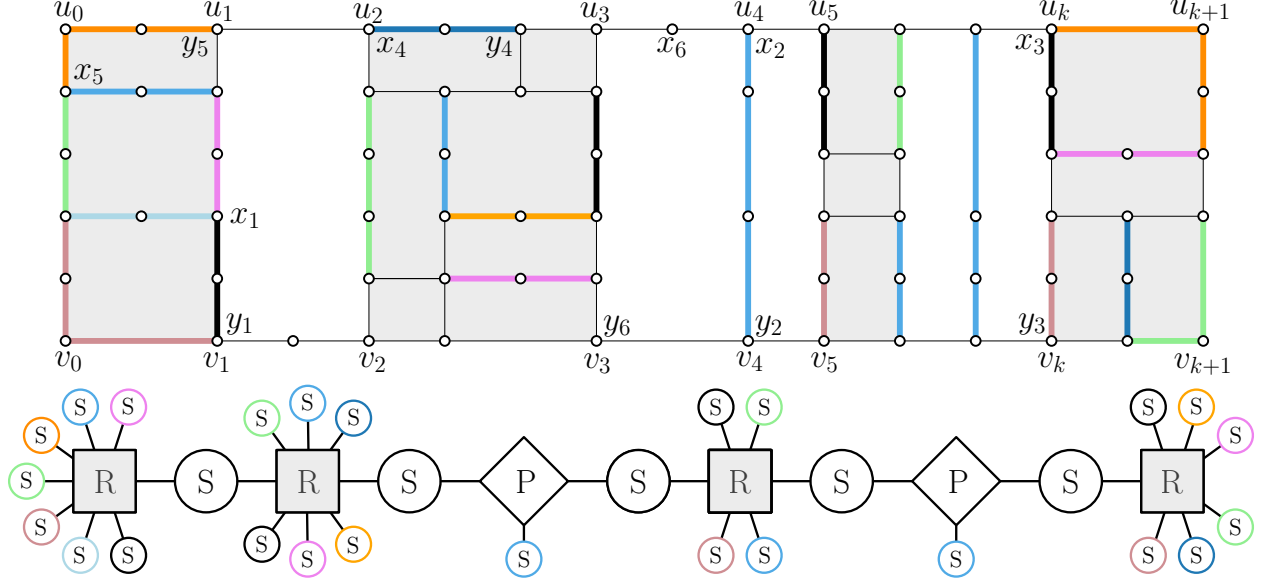


Fig. 11. A rectangular grid drawing of a planar graph and its pruned SPQR-tree T^* . S -, P -, and R -nodes are circles, rhombuses and squares, respectively. The subgraphs corresponding to S -nodes that are leaves of T^* are thick.

Case 1: there exists no separation pair $\{u, v\}$ of G such that u and v are on opposite sides of Γ_o . In this case, by Property 4, T^* contains no P -nodes. For any separation pair $\{u, v\}$ of G , we have that (i) there exist exactly two components of G with respect to $\{u, v\}$ and that (ii) exactly one of the components of G with respect to $\{u, v\}$ corresponds to an S -node, which is a simple path. This comes from Property 2 if at least one of u and v is an internal vertex, from Property 8 if u and v lie on perpendicular sides of Γ_o , and from Property 7 if u and v lie on the same side of Γ_o . It follows that there exist no two R -nodes in T . Note that T , and hence T^* , contains S -nodes, as the corners of Γ_0 are vertices of G with degree 2. Therefore, T^* is a star whose leaves are S -nodes and whose central vertex is an R -node. This proves **Condition (i)**; also, **Condition (v)** is vacuously true.

Case 2: There exists a separation pair $\{u, v\}$ of G such that u and v are on opposite sides of Γ_o . By Property 5, any other separation pair $\{u', v'\}$ different from $\{u, v\}$ where u' and v' are on opposite sides of Γ_o is such that either u and u' are on the same side of Γ_o or u and v' are on the same side of Γ_o . Therefore, after a possible rotation by a multiple of 90° , in the following we will assume that u lies on the top side of Γ_o and v lies on the bottom side of Γ_o . Let $S = [\{u_1, v_1\}, \{u_2, v_2\}, \dots, \{u_k, v_k\}]$ be the separation pairs of G such that u_1, u_2, \dots, u_k lie, in this left-to-right order, on the top side of Γ_o , such that v_1, v_2, \dots, v_k lie, in this left-to-right order, on the bottom side of Γ_o , such that all these vertices have degree 3, and such that u_i and v_i share the same x -coordinate, for $i = 1, \dots, k$. The next claim shows that $k \geq 1$.

Claim 1. *If there exists a separation pair $\{u, v\}$ of G such that u and v are on opposite sides of Γ_o , then there exists at least one separation pair $\{u', v'\}$ such that:*

- u' and v' are on opposite sides of Γ_o ;
- u' and v' share the same x -coordinate in Γ ;
- u' and v' have degree 3 in G ; and
- there exists a path between u' and v' drawn along a vertical line that is incident to an internal face of Γ .

Proof. The proof distinguishes two cases.

Suppose first that at least one of u and v , say v , has degree 3. We show that there exists a vertex u' lying along the top side of Γ_o , where possibly $u' = u$, such that the separation pair $\{u', v\}$ satisfies the properties required by the claim. Note that, since v has degree 3 and is incident to the bottom side of Γ_o , two of its

neighbors lie along the bottom side of Γ_o . Therefore, the third neighbor of v , must either be a vertex u^* incident to the top side of Γ_o (possibly $u^* = u$) or an internal vertex i_v lying vertically above v . In the former case, since Γ is rectangular, we have that u^* has degree 3, lies vertically above v in Γ (which implies that u^* and v have the same x -coordinate), and is connected to v via a path (indeed, a single edge) drawn along a vertical line. Thus, setting $u' = u^*$ yields the desired separation pair. In the latter case, since $\{u, v\}$ is a separation pair, there exists an internal face f shared by u , v , and i_v . Let u' be the first vertex of the top side of Γ_o that is encountered when traversing the boundary of f starting at v and passing through i_v . Consider the subpath of f between v and u' that contains i_v . Since i_v lies vertically above v in Γ , and since Γ is rectangular, this path must be drawn as a straight-line segment between v and u' , which implies that u' has degree 3 and has the same x -coordinate as v . Therefore, since both u' and v belong to f and lie on opposite sides of Γ_o , they form the sought separation pair.

Suppose next that both u and v have degree-2. Consider the internal face f of Γ shared by u and v . We show that there exists a separation pair that satisfies the properties of the statement whose vertices are incident to f . If f contains no degree-3 vertex incident to the top side of Γ_o and no degree-3 vertex incident to the bottom side of Γ_o , then both the paths of G that form the top and the bottom side of Γ_o belong to f , hence G is a cycle, which contradicts the assumptions of the lemma. Otherwise, f contains a degree-3 vertex u' incident to the top side of Γ_o and a vertex v' incident to the bottom side of Γ_o (or a degree-3 vertex v' incident to the bottom side of Γ_o and a vertex u' incident to the top side of Γ_o). Then the existence of the sought separation pair can be deduced as in the first case of the proof, with u' and v' playing the role of u and v . ■

We set $L = \{u_0, v_0\} \circ S \circ \{u_{k+1}, v_{k+1}\}$, where u_0, v_0, u_{k+1} , and v_{k+1} are the vertices of G lying at the top-left, bottom-left, top-right, and bottom-right corner of Γ_o , respectively, where \circ denotes the concatenation operator. For $i = 0, \dots, k+1$, let P_i be the path in G connecting u_i and v_i that is drawn along a vertical line in Γ . This path exists by the previous claim, for $i = 1, \dots, k$, and since Γ_o is a rectangle, for $i \in \{0, k+1\}$. Also, let C_i be the cycle of G that contains u_i, u_{i+1}, v_{i+1} , and v_i , that contains P_i and P_{i+1} , and that is drawn as a rectangle in Γ . Clearly, any two cycles C_i and C_{i+1} share the path P_{i+1} . We denote by G_i the subgraph of G induced by the vertices in the interior and along the boundary of C_i .

We show that T^* can be constructed iteratively starting from the empty tree, as follows. At each point of the construction, T^* will be a caterpillar whose spine does not have a P -node as an end-point. Also, a leaf of T^* will be denoted as *active* and will be used in the subsequent iteration, if any, as an attachment endpoint to extend T^* .

The construction of T^* starts by considering the following two cases.

- If $G_0 = C_0$, we introduce an S -node μ_0 in T^* . In particular, (u_1, v_1) is a virtual edge of $\text{sk}(\mu_0)$, and the other virtual edges of $\text{sk}(\mu_0)$ correspond to the edges of C_0 incident to Γ_o .
- Otherwise, $G_0 \neq C_0$. Consider a separation pair $\{u, v\}$ of G_0 . By Claim 1 applied to G_0 and since $\{u_1, v_1\}$ is the first pair in S , we have that u and v do not lie one on the top and one on the bottom side of Γ . Therefore, by Properties 2, 7 and 8, one of the two components of G_0 with respect to $\{u, v\}$ is a simple path. Thus, G_0 is the subdivision of a triconnected planar graph. Hence, we introduce an R -node μ_0 in T^* whose skeleton is obtained by replacing each maximal induced path in G_0 not containing u_1 or v_1 in its interior with a virtual edge. For each of such virtual edges that does not correspond to a single real edge, we add to T^* an S -node adjacent to μ_0 ; note that there are at least two S -nodes adjacent to μ_0 , as u_0 and v_0 have degree 2 in G . We also introduce in $\text{sk}(\mu_0)$ the virtual edge (u_1, v_1) .

In both cases (i.e., $G_0 = C_0$ and $G_0 \neq C_0$), μ_0 is the active endpoint of T^* .

Next, for $i = 1, \dots, k$, we consider the separation pair $\{u_i, v_i\}$. Denote by ξ the active endpoint of the spine (right before considering the current index i). Then ξ is either an S -node or an R -node. Also, $\text{sk}(\xi)$ contains a virtual edge (u_i, v_i) ; note that this is true for $i = 1$, as described above. As before, we distinguish two cases.

- *Suppose that $G_i = C_i$.* We have two further cases.
 - If ξ is an S -node, then we introduce a P -node $\mu_{i,1}$ in T^* adjacent to ξ and either one or two more S -nodes adjacent to $\mu_{i,1}$. In particular, the skeleton of $\mu_{i,1}$ (in T) is a bundle of three parallel edges

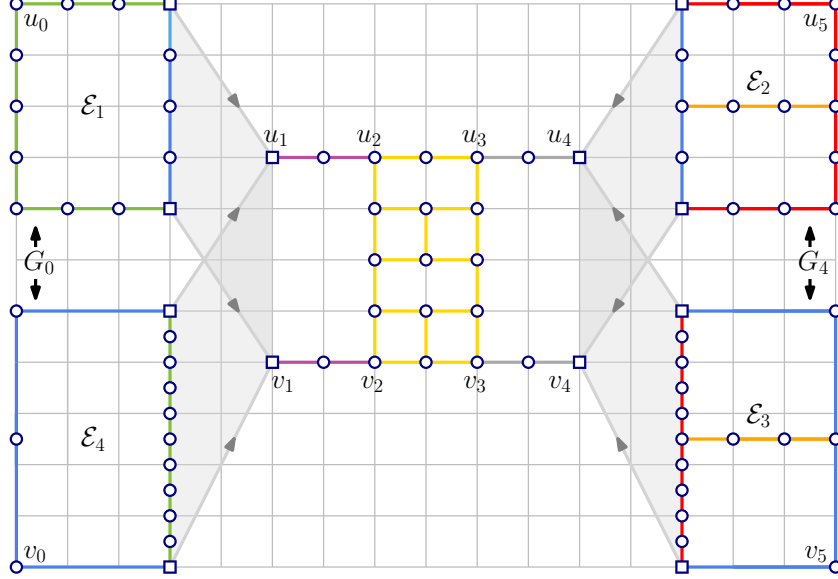


Fig. 12. Four plane embeddings of a graph G that support a rectangular drawing of G , obtained by selecting one of the plane embeddings \mathcal{E}_1 and \mathcal{E}_4 of the subgraph G_0 of G and one of the the plane embeddings \mathcal{E}_2 and \mathcal{E}_3 of the subgraph G_4 of G . Only the embeddings \mathcal{E}_1 and \mathcal{E}_2 support a unit-length rectangular drawing.

(u_i, v_i) . If P_i is a single edge, then we add to T^* a single S -node $\mu_{i,3}$ adjacent to $\mu_{i,1}$, while if P_i is not a single edge, then we add to T^* two more S -nodes $\mu_{i,2}$ and $\mu_{i,3}$ adjacent to $\mu_{i,1}$. If P_i is not a single edge, then the skeleton of $\mu_{i,2}$ is a cycle containing one virtual edge for each edge of the path P_i plus a virtual edge (u_i, v_i) . The skeleton of $\mu_{i,3}$ is a cycle consisting of a virtual edge (u_i, v_i) , followed by a virtual edge for each horizontal edge in the top side of C_i , followed by one virtual edge (u_{i+1}, v_{i+1}) , followed by a virtual edge for each horizontal edge in the bottom side of C_i . Finally, we set $\mu_{1,3}$ as the active node of T^* .

- If ξ is an R -node, then we introduce an S -node μ_i in T^* adjacent to ξ whose skeleton is a cycle consisting of a virtual edge (u_i, v_i) , followed by one virtual edge for each horizontal edge in the top side of C_i , followed by a path P^* of virtual edges defined below, followed by one virtual edge for each horizontal edge in the bottom side of C_i . If $i < k$, then the path P^* consists of the single virtual edge (u_{i+1}, v_{i+1}) ; otherwise, if $i = k$, then the path P^* contains a virtual edge for each real edge incident to the right side of Γ_o (i.e., for each edge of the right side of C_k). Finally, we set μ_i as the active endpoint of T^* .
- *Suppose now that $G_i \neq C_i$.* With the same motivation as for G_0 , we introduce an R -node μ_i in T^* adjacent to ξ whose skeleton is obtained by replacing each maximal induced path in G_i that does not contain u_i, v_i, u_{i+1} , or v_{i+1} with a virtual edge. We add an S -node for each of such virtual edges that does not correspond to a single real edge. Also, we introduce in $\text{sk}(\mu_i)$ the virtual edge (u_i, v_i) and, unless $i = k$, the virtual edge (u_{i+1}, v_{i+1}) . Finally, we set μ_i as the active endpoint of T^* .

It is easy to observe that, after each step of the inductive construction of T^* , the tree T^* is a caterpillar whose spine connects μ_0 with the active endpoint of T^* , hence T^* is eventually a caterpillar. Also, the construction guarantees that **Condition (i)** and **Condition (v)** of the statement are satisfied. \square

Consider a graph G that satisfies the conditions of Lemma 4. If the spine of the pruned SPQR-tree of G contains at least two nodes or at least one P -node, we say that G is *flat*; otherwise, G is the subdivision of a triconnected planar graph. Exploiting Lemma 4, we can prove the following; refer to Fig. 12.

Lemma 5. *Let G be an n -vertex graph. The following hold:*

- All the unit-length rectangular drawings of G , if any, have the same plane embedding \mathcal{E} (up to a reflection), which can be computed in $O(n)$ time.
- If G is flat, all the rectangular drawings of G , if any, have at most four possible plane embeddings (up to a reflection), which can be computed in $O(n)$ time.

Proof. We prove the first part of the statement.

Suppose that G has a unit-length rectangular drawing Γ . By Lemma 4, the pruned SPQR-tree T^* of G is a caterpillar. By **Condition (i)** of Lemma 4, all the nodes of T^* that are not in the spine are S -nodes, hence all the planar embeddings of G are obtained by embedding the skeletons of the P - and R -nodes of the spine of T^* .

We arbitrarily select a normal orientation T^* such that its spine is a directed path, and visit the spine μ_1, \dots, μ_k of T^* according to such an orientation. Note that neither μ_1 nor μ_k can be an S -node, by **Condition (i)** of Lemma 4 and since T does not contain any two adjacent S -nodes. We construct the plane embedding \mathcal{E} of G and select its outer face f_o as follows. All the choices we perform are obliged, as a consequence of Lemma 4 and of Properties 2 to 9.

Suppose that μ_1 is a P -node. By Property 2, the poles of μ_1 are incident to f_o . By Property 4, we have that either (i) exactly one neighbor ν of μ_1 is a Q -node, or (ii) exactly one neighbor ν of μ_1 is an S -node corresponding to a simple path in G , or (iii) at least two neighbors of μ_1 are S -nodes corresponding to a simple path in G . In cases (i) and (ii), the virtual edge of $\text{sk}(\mu_1)$ corresponding to ν must lie in between the other two virtual edges. In case (iii), since Γ is rectangular, one of the simple paths corresponding to the neighbors of μ must be shorter than the others. The corresponding virtual edge must lie in between the other virtual edges in the embedding of $\text{sk}(\mu_1)$. Two cases are possible: Either μ_1 is the unique node of the spine of T^* or not. In the former case, the virtual edges corresponding to the remaining two neighbors of μ_1 in T^* can be ordered arbitrarily. Note that this yields exactly two planar embeddings of G that are one the reflection of the other. Otherwise, we set the virtual edge corresponding to μ_2 at the rightmost virtual edge in the embedding of $\text{sk}(\mu_1)$.

Suppose that μ_1 is an R -node. Two cases are possible: Either μ_1 is the unique node of the spine of T^* or not. In the former case, G is the subdivision of a triconnected planar graph. Hence, it has a unique planar embedding \mathcal{E} , up to a reflection. Since in any unit-length rectangular drawing of G , the outer face must be bounded by a face of \mathcal{E} of maximum size and since no internal face may have the same size of the outer face, we can determine in $O(n)$ time whether \mathcal{E} does not support a rectangular drawing or whether a candidate outer face of \mathcal{E} exists. This determines a unique candidate plane embedding of G , up to a reflection. In the latter case, consider the virtual edge e_2 corresponding to μ_2 in $\text{sk}(\mu_1)$. Recall that, since μ_1 is a R -node, $\text{sk}(\mu_1)$ admits a unique (up to a reflection) planar embedding. In such an embedding, we remove the edge $e_1 = (u_1, v_1)$, and let $\text{sk}^-(\mu_1)$ be the resulting embedded graph. Note that, by **Condition (i)** of Lemma 4, each virtual edge of $\text{sk}^-(\mu_1)$ corresponds to a simple path in G . Let G^- be the embedded subgraph of G obtained by replacing each virtual edge of $\text{sk}^-(\mu_1)$ with the associated path. Let P and P_1 be the two paths of G^- between u_1 and v_1 that share the same face of G^- (note that, they stem from the face of $\text{sk}^-(\mu_1)$ that used to host the edge e_1). Since Γ is unit-length and rectangular, one of P and P_1 , say P_1 , is shorter than the other. We select the embedding of $\text{sk}(\mu_1)$ so that the path of $\text{sk}(\mu_1)$ that corresponds to P_1 is incident to the right outer face of the embedding of $\text{sk}(\mu_1)$.

Consider now a node μ_i , with $1 < i < k$. Let e_{i-1} and let e_i be the virtual edges of $\text{sk}(\mu_i)$ corresponding to μ_{i-1} and μ_{i+1} . If μ_i is an S -node, then there is no embedding choice to perform. Otherwise, we exploit the following observation. Since a rectangular drawing of G is convex, the separation pairs corresponding to the poles of P - and R -nodes must be incident to the outer face of any rectangular drawing of G [20,36]. Therefore, the embedding choices for μ_i are described below.

Suppose that μ_i is a P -node. Let ν be the neighbor of μ_i different from μ_{i-1} and μ_{i+1} . By Property 4, we have that either (i) ν is a Q -node, or (ii) ν is an S -node corresponding to a simple path in G . In both cases, the virtual edge of $\text{sk}(\mu_i)$ corresponding to ν lies in between e_{i-1} and e_i . Also, we let e_{i-1} and e_i be the leftmost and the rightmost virtual edges in the embedding of $\text{sk}(\mu_i)$, respectively.

Suppose that μ_i is an R -node. Recall that, since μ_i is an R -node, $\text{sk}(\mu_i)$ admits a unique (up to a reflection) planar embedding. We select the embedding of $\text{sk}(\mu_i)$ so that e_{i-1} and e_i are incident to the left outer face and to the right outer face of such an embedding, respectively.

Finally, consider now the node μ_k . The embedding of $\text{sk}(\mu_k)$ can be selected, based on its type, as described for μ_1 .

Now, we prove the second part of the statement. Recall that the separation pairs corresponding to the poles of P - and R -nodes must be incident to the outer face of any rectangular drawing of G . Therefore, the embedding choices for the P - and R -nodes μ_i , with $1 < i < k$, in an embedding that supports a rectangular drawing are obliged and correspond to the ones described above. Also, for the S -nodes there are no embedding choices. Therefore, the only remaining embedding choices occur on μ_1 and μ_k .

If $k = 1$, then the spine of T^* contains a single node. If $\mu_1 = \mu_k$ is an R -node, then G is not flat and it is the subdivision of a triconnected planar graph and there is nothing to prove. Otherwise, $\mu_1 = \mu_k$ is a P -node, and G consists of three paths sharing their end-vertices. Therefore, it admits three plane embeddings, up to a reflection.

If $k > 1$, consider node μ_1 . If μ_1 is an R -node, then consider the subgraph G_0 of G corresponding to it. Namely, let e_{μ_1, μ_2} the virtual edge of $\text{sk}(\mu_2)$ corresponding to μ_1 , then $G_0 = \exp(e_{\mu_1, \mu_2})$. As shown above, G_0 is the subdivision of a triconnected planar graph. Since it admits a unique planar embedding (up to a reflection), since there exists a unique face of such an embedding that contains the poles of μ_1 , and since these vertices must be incident to the outer face of a plane embedding of G that supports a rectangular drawing of G , we have that G_0 admits only two candidate plane embeddings. If μ_1 is a P -node, then let ν_1 , ν_2 , and ν_3 be its three neighbors (see Lemma 4) and let ν_3 be its neighbor in the spine of T^* . By Lemma 4, ν_1 and ν_2 are S -nodes whose corresponding subgraph of G is a simple path, whereas the subgraph of G corresponding to ν_3 is not a simple path. Note that, because any rectangular drawing is also convex, the embedding \mathcal{E}_1 of $\text{sk}(\mu_1)$ induced by any embedding of G that supports a rectangular drawing is such that the virtual edge corresponding to ν_3 is incident to the outer face of \mathcal{E}_1 . It follows that the only two possible choices to determine a candidate embedding of $\text{sk}(\mu_1)$ depend on the fact that the virtual edge corresponding to ν_1 is before or after the virtual edge corresponding to ν_2 . The degrees of freedom of the embeddings of $\text{sk}(\mu_k)$ are analogous. Hence, if $k \neq 1$, we have four possible plane embeddings of G , up to a reflection. \square

The next theorem shows that the UR problem is polynomial-time solvable. Surprisingly, the problem seems to be harder for non-flat instances.

Theorem 6. *The UNIT-LENGTH RECTANGULAR problem is cubic-time solvable. Also, if the input planar graph is flat, then the UNIT-LENGTH RECTANGULAR problem is linear-time solvable.*

Proof. First, we test whether G satisfies the conditions of Lemma 4, which can clearly be done in $O(n)$ time, where n is the number of vertices of G , by computing and visiting T^* . We reject the instance if this test fails.

If G is not flat, then the spine of T^* consists of a single R -node, by definition, hence G is the subdivision of a triconnected planar graph and it admits a unique planar embedding, up to reflection. Hence, we can test whether G admits a unit-length rectangular drawing in $O(n^3)$ time by means of Theorem 5.

If G is flat, then, by means of Lemma 5, we compute in $O(n)$ time the unique candidate plane embedding \mathcal{E} of G that may support a unit-length rectangular drawing of G , if any. Let f_o be the outer face of \mathcal{E} . We show that there exists a unique candidate drawing Γ_o of f_o , that is, in any unit-length rectangular drawing of G the outer face is delimited by the same rectangle Γ_o , up to a reflection and a rotation. Provided this statement, we can use Theorem 3 to test in $O(n)$ time for the existence of a unit-length rectangular drawing of G that respects the plane embedding \mathcal{E} and such that f_o is drawn as Γ_o .

We now show that there exists a unique candidate drawing Γ_o of f_o . We distinguish two cases, depending on whether the spine of T^* contains a P -node (**Case 1**) or not (**Case 2**). In **Case 1**, let μ be a P -node of the spine of T^* , and let u and v be the poles of μ . By Property 4, these vertices lie on opposite sides of the rectangle Γ_o bounding the outer face of any rectangular drawing Γ of G and there exists exactly one component of G with respect to $\{u, v\}$ that is a simple path P whose vertices are drawn on a straight line in Γ . In **Case 2**, let μ be an R -node of the spine of T^* , and let u and v be the poles of μ . Since the spine

of T^* does not contain any P -node and since it is not a single R-node, there exists a neighbor ν of μ in the spine of T^* that is an S -node. By Property 6, vertices u and v lie on opposite sides of the rectangle Γ_o bounding the outer face of any rectangular drawing Γ and there exists a path P between u and v that belongs to the component of G with respect to $\{u, v\}$ corresponding to μ ; also, the path P is incident to an internal face of Γ and its vertices are drawn on a straight line. Both in **Case 1** and in **Case 2**, let $|P|$ and $|f_o|$ denote the length of P and f_o , respectively. By Property 4, up to a 90° rotation of Γ , the value $|P|$ must correspond to the height of Γ , whereas $(|f_o| - 2|P|)/2$ must correspond to the width of Γ . Note that, if the latter value is less than or equal to zero, then G does not admit any unit-length rectangular drawing, in which case we reject the instance. Let r (resp. ℓ) be the number of edges traversed when walking in clockwise (resp. counter-clockwise) direction from u and v along the cycle C_o bounding f_o . By the above discussion, the four vertices $u_r, v_r, v_\ell,$ and u_ℓ that lie at the corners of the rectangle Γ_o bounding the outer face of any rectangular drawing Γ of G are the vertices at distance $(r - |P|)/2, (r + |P|)/2, r + (\ell - |P|)/2$ and $r + (\ell + |P|)/2$ in clockwise direction from u along C_o . It follows that Γ_o is uniquely defined, which proves the statement and hence the theorem. \square

The techniques we developed for unit-length drawings allow us to prove the following.

Theorem 7. *The problem of testing for the existence of a rectangular drawing of an n -vertex planar graph G is solvable in $O(n^2 \log^3 n)$ time. Also, if G is flat, the problem is solvable in $O(n \log^3 n)$ time.*

Proof. First, we test whether G satisfies the conditions of Lemma 4, which can clearly be done in $O(n)$ time by computing and visiting T^* , and reject the instance if this test fails.

We start by considering the case in which G is flat. Due to Lemma 5, only up to four plane embeddings of G are candidates for a rectangular drawing of G that respects them. Also, such embeddings can be computed in $O(n)$ time. For each of them, we test for the existence of a rectangular drawing respecting it by solving a max-flow problem on a linear-size planar network with multiple sources and sinks in $O(n \log^3 n)$ time [11]. Such a network can be defined following Tamassia's [16] classic approach to test for the existence of rectilinear drawings of plane graphs. In such a network \mathcal{N} , we have that:

- each node of \mathcal{N} corresponding to a vertex of G is a source producing 4 units of flow, each corresponding to a 90° angle;
- each node of \mathcal{N} corresponding to a face f of G is a sink consuming $2|f| - 4$ (resp. $2|f| + 4$) units of flow if f is an internal face (resp. the outer face) of G , where $|f|$ is the length of f ;
- each node of \mathcal{N} corresponding to a vertex of G has an outgoing arc directed toward the nodes corresponding to its incident faces; and
- each arc of \mathcal{N} has a lower bound of 1 unit of flow.

The existence of a flow in \mathcal{N} from the sources to the sinks with value $4n$ corresponds to the existence of a rectilinear drawing of G that respects its plane embedding. It is easy to modify \mathcal{N} so that the existence of a flow with value $4n$ corresponds to the existence of a rectangular drawing of G . Namely, it suffices to equip each arc of \mathcal{N} with an upper bound of 2 (resp. 3) if the node of \mathcal{N} the arc is incident to corresponds to an internal face (resp. the outer face) of G , and with a lower bound of 1 (resp. 2) if the node of \mathcal{N} the arc is incident to corresponds to an internal face (resp. the outer face) of G . The existence of a flow of value $4n$ in \mathcal{N} can be tested by using the max-flow algorithm of Borradaile et al. [11].

If G is not flat, then G is the subdivision of a triconnected planar graph. Let \mathcal{E} be the unique planar embedding of G . For each possible selection of a face of \mathcal{E} as the outer face, we consider the resulting plane embedding of G and use the same strategy as above to test for the existence of a rectilinear drawing of G that respects such a plane embedding. Since there are $O(n)$ possible choices of the outer face, this results in an $O(n^2 \log^3 n)$ -time algorithm. \square

6 Conclusions and Open Problems

We studied the recognition of graphs admitting the beautiful drawings that require rectilinear edges of unit length, planarity, and convexity of the faces. We showed that, if the outer face is required to be drawn as

a rectangle, the problem is polynomial-time solvable, while it is NP-hard if the outer face is an arbitrary polygon, even if the input is biconnected, unless such a polygon is specified in advance. These results hold both in the fixed-embedding and in the variable-embedding settings. A byproduct of our results is a polynomial-time algorithm to recognize graphs admitting a rectangular (non-necessarily unit-length) drawing.

It is worth remarking that if the input is a subdivision of a triconnected planar graph, then our algorithms pay an extra time to handle the outer face. Specifically, for unit-length rectangular drawings, an extra quadratic time is used to guess a rectangular drawing of the unique candidate outer face, while, for general rectangular drawings, an extra linear time is used to determine the actual candidate outer face. Hence, it is appealing to study efficient algorithms for this specific case. Observe that the NP-hardness results on trees in [9,28] heavily rely on the variable embedding setting.

References

1. Abel, Z., Demaine, E.D., Demaine, M.L., Eisenstat, S., Lynch, J., Schardl, T.B.: Who needs crossings? Hardness of plane graph rigidity. In: Fekete, S.P., Lubiw, A. (eds.) 32nd International Symposium on Computational Geometry (SoCG '16). LIPIcs, vol. 51, pp. 3:1–3:15. Schloss Dagstuhl - Leibniz-Zentrum für Informatik (2016). <https://doi.org/10.4230/LIPIcs.SocG.2016.3>
2. Alegría, C., Da Lozzo, G., Di Battista, G., Frati, F., Grosso, F., Patrignani, M.: Unit-length rectangular drawings of graphs. In: Angelini, P., von Hanxleden, R. (eds.) Graph Drawing and Network Visualization - 30th International Symposium, GD 2022, Tokyo, Japan, September 13-16, 2022, Revised Selected Papers. Lecture Notes in Computer Science, vol. 13764, pp. 127–143. Springer (2022). https://doi.org/10.1007/978-3-031-22203-0_10, https://doi.org/10.1007/978-3-031-22203-0_10
3. Alegría, C., Borrazzo, M., Da Lozzo, G., Di Battista, G., Frati, F., Patrignani, M.: Testing the planar straight-line realizability of 2-trees with prescribed edge lengths. *European Journal of Combinatorics* p. 103806 (2023). <https://doi.org/https://doi.org/10.1016/j.ejc.2023.103806>, <https://www.sciencedirect.com/science/article/pii/S0195669823001233>
4. Angelini, P., Da Lozzo, G., Bartolomeo, M.D., Di Battista, G., Hong, S., Patrignani, M., Roselli, V.: Anchored drawings of planar graphs. In: Duncan, C.A., Symvonis, A. (eds.) Graph Drawing - GD 2014. Lecture Notes in Computer Science, vol. 8871, pp. 404–415. Springer (2014). https://doi.org/10.1007/978-3-662-45803-7_34
5. Angelini, P., Da Lozzo, G., Frati, F., Lubiw, A., Patrignani, M., Roselli, V.: Optimal morphs of convex drawings. In: Arge, L., Pach, J. (eds.) 31st International Symposium on Computational Geometry, SoCG 2015, June 22-25, 2015, Eindhoven, The Netherlands. LIPIcs, vol. 34, pp. 126–140. Schloss Dagstuhl - Leibniz-Zentrum für Informatik (2015). <https://doi.org/10.4230/LIPIcs.SocG.2015.126>
6. Asgharian-Sardroud, A., Bagheri, A.: Embedding cycles and paths on solid grid graphs. *J. Supercomput.* **73**(4), 1322–1336 (2017). <https://doi.org/10.1007/s11227-016-1811-y>
7. Beck, M., Storandt, S.: Puzzling grid embeddings. In: Blelloch, G.E., Finocchi, I. (eds.) Proceedings of the Symposium on Algorithm Engineering and Experiments, ALENEX 2020, Salt Lake City, UT, USA, January 5-6, 2020. pp. 94–105. SIAM (2020)
8. de Berg, M., Khosravi, A.: Optimal binary space partitions for segments in the plane. *International Journal of Computational Geometry & Applications* **22**(03), 187–205 (2012). <https://doi.org/10.1142/S0218195912500045>
9. Bhatt, S.N., Cosmadakis, S.S.: The complexity of minimizing wire lengths in VLSI layouts. *Inf. Process. Lett.* **25**(4), 263–267 (1987). [https://doi.org/10.1016/0020-0190\(87\)90173-6](https://doi.org/10.1016/0020-0190(87)90173-6)
10. Biedl, T.C., Kant, G.: A better heuristic for orthogonal graph drawings. *Comput. Geom.* **9**(3), 159–180 (1998). [https://doi.org/10.1016/S0925-7721\(97\)00026-6](https://doi.org/10.1016/S0925-7721(97)00026-6)
11. Borradaile, G., Klein, P.N., Mozes, S., Nussbaum, Y., Wulff-Nilsen, C.: Multiple-source multiple-sink maximum flow in directed planar graphs in near-linear time. *SIAM J. Comput.* **46**(4), 1280–1303 (2017). <https://doi.org/10.1137/15M1042929>
12. Cabello, S., Demaine, E.D., Rote, G.: Planar embeddings of graphs with specified edge lengths. *Journal of Graph Algorithms and Applications* **11**(1), 259–276 (2007). <https://doi.org/10.7155/jgaa.00145>
13. Chang, Y., Yen, H.: On bend-minimized orthogonal drawings of planar 3-graphs. In: 33rd International Symposium on Computational Geometry, SoCG 2017, July 4-7, 2017, Brisbane, Australia. pp. 29:1–29:15 (2017). <https://doi.org/10.4230/LIPIcs.SocG.2017.29>
14. Cornelsen, S., Karrenbauer, A.: Accelerated bend minimization. *J. Graph Algorithms Appl.* **16**(3), 635–650 (2012). <https://doi.org/10.7155/jgaa.00265>

15. Devillers, O., Liotta, G., Preparata, F.P., Tamassia, R.: Checking the convexity of polytopes and the planarity of subdivisions. *Comput. Geom.* **11**(3-4), 187–208 (1998). [https://doi.org/10.1016/S0925-7721\(98\)00039-X](https://doi.org/10.1016/S0925-7721(98)00039-X)
16. Di Battista, G., Eades, P., Tamassia, R., Tollis, I.G.: *Graph Drawing: Algorithms for the Visualization of Graphs*. Prentice-Hall (1999)
17. Di Battista, G., Liotta, G., Vargiu, F.: Spirality and optimal orthogonal drawings. *SIAM J. Comput.* **27**(6), 1764–1811 (1998). <https://doi.org/10.1137/S0097539794262847>
18. Di Battista, G., Tamassia, R.: On-line maintenance of triconnected components with SPQR-trees. *Algorithmica* **15**(4), 302–318 (1996). <https://doi.org/10.1007/BF01961541>
19. Di Battista, G., Tamassia, R.: On-line planarity testing. *SIAM J. Comput.* **25**(5), 956–997 (1996)
20. Di Battista, G., Tamassia, R., Vismara, L.: Incremental convex planarity testing. *Inf. Comput.* **169**(1), 94–126 (2001). <https://doi.org/10.1006/inco.2001.3031>
21. Didimo, W., Kaufmann, M., Liotta, G., Ortali, G.: Rectilinear planarity testing of plane series-parallel graphs in linear time. In: Auber, D., Valtr, P. (eds.) *Graph Drawing and Network Visualization*, 2020. LNCS, vol. 12590, pp. 436–449. Springer (2020)
22. Didimo, W., Liotta, G., Ortali, G., Patrignani, M.: Optimal orthogonal drawings of planar 3-graphs in linear time. In: Chawla, S. (ed.) *Proc. ACM-SIAM Symposium on Discrete Algorithms (SODA '20)*. pp. 806–825. ACM-SIAM (2020). <https://doi.org/https://doi.org/10.1137/1.9781611975994.49>
23. Eades, P., Wormald, N.C.: Fixed edge-length graph drawing is NP-hard. *Disc. Appl. Math.* **28**(2), 111–134 (1990). [https://doi.org/10.1016/0166-218X\(90\)90110-X](https://doi.org/10.1016/0166-218X(90)90110-X)
24. Felsner, S.: Rectangle and square representations of planar graphs. In: Pach, J. (ed.) *Thirty Essays on Geometric Graph Theory*, pp. 213–248. Springer New York, New York, NY (2013). https://doi.org/10.1007/978-1-4614-0110-0_12
25. Frati, F.: Planar rectilinear drawings of outerplanar graphs in linear time. *Comput. Geom.* **103**, 101854 (2022). <https://doi.org/10.1016/J.COMGEO.2021.101854>, <https://doi.org/10.1016/j.comgeo.2021.101854>
26. Garg, A., Liotta, G.: Almost bend-optimal planar orthogonal drawings of biconnected degree-3 planar graphs in quadratic time. In: *Graph Drawing, 7th International Symposium, GD'99, Stirin Castle, Czech Republic, September 1999, Proceedings*. pp. 38–48 (1999). https://doi.org/10.1007/3-540-46648-7_4
27. Garg, A., Tamassia, R.: On the computational complexity of upward and rectilinear planarity testing. *SIAM J. Comput.* **31**(2), 601–625 (2001). <https://doi.org/10.1137/S0097539794277123>
28. Gregori, A.: Unit-length embedding of binary trees on a square grid. *Information Processing Letters* **31**(4), 167–173 (1989). [https://doi.org/10.1016/0020-0190\(89\)90118-X](https://doi.org/10.1016/0020-0190(89)90118-X)
29. Gupta, S., Sa'ar, G., Zehavi, M.: Grid recognition: Classical and parameterized computational perspectives. *Journal of Computer and System Sciences* **136**, 17–62 (2023). <https://doi.org/https://doi.org/10.1016/j.jcss.2023.02.008>, <https://www.sciencedirect.com/science/article/pii/S0022000023000259>
30. Gutwenger, C., Mutzel, P.: A linear time implementation of SPQR-trees. In: Marks, J. (ed.) *Graph Drawing, 8th International Symposium, GD 2000, Colonial Williamsburg, VA, USA, September 20-23, 2000, Proceedings*. LNCS, vol. 1984, pp. 77–90. Springer (2000). https://doi.org/10.1007/3-540-44541-2_8
31. Hasan, M.M., Rahman, M.S.: No-bend orthogonal drawings and no-bend orthogonally convex drawings of planar graphs (extended abstract). In: *COCOON. Lecture Notes in Computer Science*, vol. 11653, pp. 254–265. Springer (2019)
32. Itai, A., Papadimitriou, C.H., Szwarcfiter, J.L.: Hamilton paths in grid graphs. *SIAM Journal on Computing* **11**(4), 676–686 (1982). <https://doi.org/10.1137/0211056>
33. Kant, G.: Drawing planar graphs using the canonical ordering. *Algorithmica* **16**(1), 4–32 (1996). <https://doi.org/10.1007/BF02086606>
34. Liu, Y., Morgana, A., Simeone, B.: A linear algorithm for 2-bend embeddings of planar graphs in the two-dimensional grid. *Discrete Applied Mathematics* **81**(1-3), 69–91 (1998). [https://doi.org/10.1016/S0166-218X\(97\)00076-0](https://doi.org/10.1016/S0166-218X(97)00076-0)
35. Miura, K., Haga, H., Nishizeki, T.: Inner rectangular drawings of plane graphs. *International Journal of Computational Geometry and Applications* **16**(2-3), 249–270 (2006). <https://doi.org/10.1142/S0218195906002026>
36. Nishizeki, T., Rahman, M.S.: *Planar Graph Drawing, Lecture Notes Series on Computing*, vol. 12. World Scientific (2004). <https://doi.org/10.1142/5648>
37. Nishizeki, T., Rahman, M.S.: Rectangular drawing algorithms. In: Tamassia, R. (ed.) *Handbook on Graph Drawing and Visualization*, pp. 317–348. Chapman and Hall/CRC (2013)
38. Rahman, M.S., Egi, N., Nishizeki, T.: No-bend orthogonal drawings of series-parallel graphs. In: Healy, P., Nikolov, N.S. (eds.) *Graph Drawing, 13th International Symposium, GD 2005, Limerick, Ireland, September 12-14, 2005, Revised Papers. Lecture Notes in Computer Science*, vol. 3843, pp. 409–420. Springer (2005). https://doi.org/10.1007/11618058_37

39. Rahman, M.S., Egi, N., Nishizeki, T.: No-bend orthogonal drawings of subdivisions of planar triconnected cubic graphs. *IEICE Transactions* **88-D**(1), 23–30 (2005)
40. Rahman, M.S., Nakano, S., Nishizeki, T.: Rectangular grid drawings of plane graphs. *Comput. Geom.* **10**(3), 203–220 (1998). [https://doi.org/10.1016/S0925-7721\(98\)00003-0](https://doi.org/10.1016/S0925-7721(98)00003-0)
41. Rahman, M.S., Nakano, S., Nishizeki, T.: A linear algorithm for bend-optimal orthogonal drawings of triconnected cubic plane graphs. *J. Graph Algorithms Appl.* **3**(4), 31–62 (1999), <http://www.cs.brown.edu/publications/jgaa/accepted/99/SaidurNakanoNishizeki99.3.4.pdf>
42. Rahman, M.S., Nishizeki, T.: Bend-minimum orthogonal drawings of plane 3-graphs. In: *Graph-Theoretic Concepts in Computer Science, 28th International Workshop, WG 2002, Cesky Krumlov, Czech Republic, June 13-15, 2002, Revised Papers*. pp. 367–378 (2002). https://doi.org/10.1007/3-540-36379-3_32
43. Rahman, M.S., Nishizeki, T., Ghosh, S.: Rectangular drawings of planar graphs. *J. Algorithms* **50**(1), 62–78 (2004). [https://doi.org/10.1016/S0196-6774\(03\)00126-3](https://doi.org/10.1016/S0196-6774(03)00126-3)
44. Rahman, M.S., Nishizeki, T., Naznin, M.: Orthogonal drawings of plane graphs without bends. *J. Graph Algorithms Appl.* **7**(4), 335–362 (2003), <http://jgaa.info/accepted/2003/Rahman+2003.7.4.pdf>
45. Schaefer, M.: Realizability of graphs and linkages. In: Pach, J. (ed.) *Thirty Essays on Geometric Graph Theory*, pp. 461–482. Springer New York, New York, NY (2013). https://doi.org/10.1007/978-1-4614-0110-0_24
46. Storer, J.A.: The node cost measure for embedding graphs on the planar grid (extended abstract). In: Miller, R.E., Ginsburg, S., Burkhard, W.A., Lipton, R.J. (eds.) *Proceedings of the 12th Annual ACM Symposium on Theory of Computing, April 28-30, 1980, Los Angeles, California, USA*. pp. 201–210. ACM (1980). <https://doi.org/10.1145/800141.804667>
47. Tamassia, R.: On embedding a graph in the grid with the minimum number of bends. *SIAM J. Comput.* **16**(3), 421–444 (1987). <https://doi.org/10.1137/0216030>
48. Tarjan, R.E.: Depth-first search and linear graph algorithms. *SIAM J. Comput.* **1**(2), 146–160 (1972). <https://doi.org/10.1137/0201010>, <https://doi.org/10.1137/0201010>
49. Thomassen, C.: Plane representations of graphs. In: Bondy, J., Murty, U. (eds.) *Progress in Graph Theory*, pp. 43–69. Academic Press, Toronto, Orlando (1987)
50. Ungar, P.: On Diagrams Representing Maps. *Journal of the London Mathematical Society* **s1-28**(3), 336–342 (Jul 1953). <https://doi.org/10.1112/jlms/s1-28.3.336>
51. Vijayan, G., Wigderson, A.: Rectilinear graphs and their embeddings. *SIAM Journal on Computing* **14**(2), 355–372 (1985)
52. Zhou, X., Nishizeki, T.: Orthogonal drawings of series-parallel graphs with minimum bends. *SIAM J. Discrete Math.* **22**(4), 1570–1604 (2008). <https://doi.org/10.1137/060667621>